ORIGINAL RESEARCH **Open access**

Short-Term Residential Load Forecasting Using a Hybrid Statistical and Machine Learning Approach

Petra Novak[1*], Milan Horvat[2], Jakub Vesely[1], Jana Kralova[2]

Abstract

The dependable operation of contemporary power grids hinges on accurate short-term load forecasting, which underpins efficient energy dispatch and fortifies system reliability against growing consumption and climatic unpredictability. To tackle the problem of projecting residential electricity use, we put forward SSRXLR—an original hybrid construct that brings together statistical and machine learning components: a sparse Seasonal Autoregressive Integrated Moving Average Exogenous formulation, Random Forest, Extreme Gradient Boosting, Long Short-Term Memory, and a Residual Correction procedure, so capturing both linear trends and complex nonlinear interactions. One year of high-resolution (5-minute-step) energy and weather observations from a Las Vegas, Nevada household formed the basis of our analysis. A rigorous variable selection exercise singled out four dominant drivers: sea level pressure, temperature, feels-like temperature, and dew point. The resulting methodology turned in powerful predictive results when measured against multiple performance indicators. Benchmarked alongside well-established alternatives, our approach registered a root mean square logarithmic error of 0.043, which amounts to an RMSLE reduction advantage of 0.066 over Random Forest and 0.106 over the Seasonal Autoregressive Integrated Moving Average Exogenous model. The coefficient of determination reached 0.97 for our method, exceeding the figures posted by Random Forest (0.92) and the Seasonal Autoregressive Integrated Moving Average Exogenous model (0.67). What these findings underscore is the considerable benefit of marrying advanced statistical modeling with machine learning and careful predictor selection for high-fidelity short-term load forecasting. The framework we describe offers an extensible platform suitable for smart grid orchestration, resource scheduling, and renewable integration across a range of deployment environments.

Keywords Machine learning, Artificial intelligence, Electrical load forecasting, Statistical analysis, Energy consumption, Power grid, Remainder predicting

*Correspondence:
Petra Novak
petra.novak@cvut.cz
[1] Department of Intelligent Power Networks, Faculty of Electrical Engineering, Czech Technical University, Prague, Czech Republic
[2] Department of AI and Energy Informatics, Faculty of Informatics, Comenius University, Bratislava, Slovakia

Introduction

Energy generation requirements are steadily rising due to ongoing population growth and industrial expansion [1-3]. For producers, this means that projecting the necessary energy output with precision has become indispensable to maintaining supply efficiency. When viewed from the grid perspective, such projections serve purposes well beyond simple volume estimation—they enable optimal protection of equipment, efficient operational routines (e.g., distance relay [4, 5]), strengthened reliability and resilience [6, 7], predictive maintenance scheduling [8, 9], electricity price forecasting [10-12], load consumption prediction [13, 14], and other critical functions.

This is an open access article distributed under the terms of the Creative Commons Attribution-NonCommercial-ShareAlike 4.0 International License (CC BY-NC-SA 4.0), which permits non-commercial use, distribution, reproduction, and adaptation in any medium or format, provided that appropriate credit is given to the original author(s) and source, a link to the license is provided, and any changes made are indicated. Adapted material must be distributed under the same license.

© 2023 The Author(s). | Published by Institute of Smart Energy Systems Press

The core concern of the present study is load prediction. Load forecasting efforts are conventionally divided into three temporal categories: Long-Term Load Forecasting (LTLF) [15], Mid-Term Load Forecasting (MTLF) [16], and Short-Term Load Forecasting (STLF) [17]. Strategic planning and capital investment depend heavily on the far-reaching perspectives that LTLF supplies regarding distant future energy needs. MTLF, by contrast, concentrates on demand projections spanning months to a year, equipping utilities to adapt resource allocation in response to seasonal shifts. STLF—the primary emphasis of our work—targets energy requirement estimates over compact horizons of a week or less, thereby allowing daily demand to be met through appropriately calibrated distribution. Adopting this structured framing lets us confront specific difficulties and strengthen energy management and distribution architectures, with particular relevance to STLF.

Forecast accuracy can suffer substantially when the underlying data are sparse or of poor quality. Limited availability and substandard data each act to degrade precision. The forecasting task is made more formidable still by fluctuating influences—meteorological conditions, economic variability, and occupant behavior—most acutely through seasonal rhythms and weather-sensitive consumption patterns. Nonlinear linkages among contributory variables create additional hurdles for both statistical techniques and machine learning models. Maintaining grid stability, however, depends squarely on trustworthy load predictions. Patterns of end-user behavior and the growing penetration of renewable generation can each dramatically shift demand forecasts. Moreover, newly developed forecasting tools must integrate smoothly into existing operational frameworks, a requirement that calls for considerable computational capacity and scalability if complex power systems are to be managed effectively [18, 19].

Worldwide energy appetite has climbed without interruption across the last century and a half, propelled by rapid demographic expansion and industrial development [20]. Forecasting practice has long drawn on parametric statistical approaches [21, 22]. As one representative example, the quantile regression averaging technique set out in Liu *et al*. [23] demonstrated enhanced prediction intervals when measured against benchmarks, using material from the GEFCom2014 probabilistic load forecasting track.

An extensive review presented in Kuster *et al*. [24] examined 113 application instances distributed over 41 studies dealing with electrical load forecasting via parametric statistical tools—among them Autoregressive Integrated Moving Average (ARIMA), regression, and Autoregressive Moving Average (ARMA). The review highlighted the effectiveness of these tools and identified regression as especially well adapted to long-term load forecasting (LTLF). Time-series formulations such as ARIMA have shown themselves capable of delivering strong accuracy within forecasting settings [25].

The work reported in Haq and Ni [26] advanced a hybrid STLF model rooted in time-series analysis, trialed through a case study situated in Houston, Texas, USA. The model recorded MAPE readings of 4.11 for January-March, 4.62 for April-June, 3.98 for July-September, and 5.46 for October-December. Despite the difficulties posed by nonlinear relationships, parametric statistical methods—regression [27], ARIMA [28], and Seasonal ARIMA (SARIMA) [29] among them—rest on well-established theoretical foundations and have seen broad adoption [30, 31].

Explorations of machine learning (ML) for STLF have likewise been undertaken. A multi-scale convolutional neural network (MS-CNN) described in Deng *et a*l. [32] delivered MAPE improvements of 34.73 %, 14.22 %, and 19.05 % when placed alongside Recursive Multi-Step LSTMs (RM-LSTMs), Direct Multi-Step MS-CNNs (DM-MS-CNNs), and Direct Multi-Step GCNNs (DM-GCNNs), respectively. In a related vein, Lin *et al*. [33] put forward a Graph Neural Network (GNN)-based STLF approach. At the same time, the outcomes proved promising; the technique's reliability was contingent on having access to sizable stores of uniform-length historical data.

When applied to monthly and weekly load forecasting, Artificial Neural Networks (ANNs) have been found to outperform multiple linear regression (MLR). The figures reported in Mir *et al.* [34] bear this out: min monthly MAPE = 2.293% and min monthly RMSE = 24.71 for ANNs, set against min monthly MAPE = 2.651% and min monthly RMSE = 36.81 for MLR. Elsewhere, Sharma and Jain [35] described a two-stage design blending Backpropagation Neural Networks (BPNNs) with

© 2023 The Author(s). | Published by Institute of Smart Energy Systems Press

Radial Basis Function Neural Networks (RBFNNs); the resulting RMSE stood at 302.67 for average load and 432 for peak load, placing it ahead of both ARIMA and LSTM models.

An investigation centered on New York City [36] pitted four forecasting methods against one another, yielding Mean Squared Error (MSE) values of 966 for linear regression, 135 for random forest regressor, 173 for gradient boosting regressor, and 169 for neural network. Of the four, the random forest regressor—an ML technique—displayed the greatest accuracy.

Despite the breadth of research effort, applying ML methods to load forecasting still presents several persistent challenges. Difficulties surrounding complex model integration, computational burden, interpretability, and generalizability all remain live concerns. As noted above, data quality also continues to shape model effectiveness. Taken together, the research gaps evident across the full spectrum of load forecasting categories are brought together in **Figure 1.**

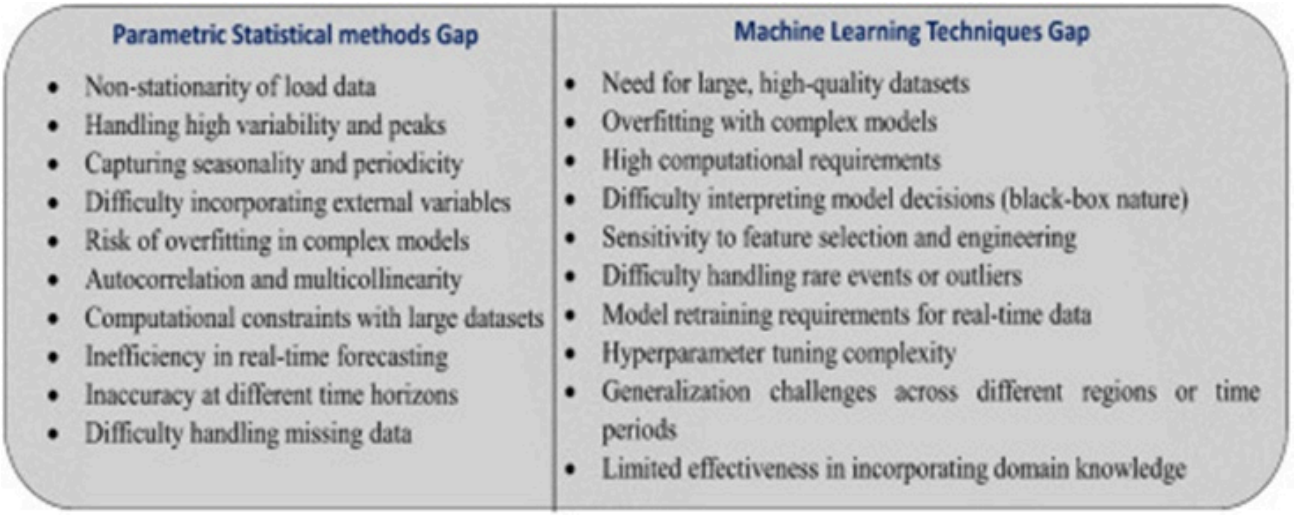

Figure 1. Challenges of Statistical and ML Load Forecasting.

The research community has pursued diverse strategies to surmount the obstacles that characterize load forecasting. Among these are deep learning architectures [37], frameworks that couple Generalized Additive Models with ARIMA [38], integrated ARIMA–SVM formulations [39], and unified LSTM–SARIMAX designs [40]. A representative illustration can be drawn from work that paired Long Short-Term Memory (LSTM) with Support Vector Regression (SVR); estimating electrical load consumption through this combination produced RMSE metrics spanning a maximum of 3, a minimum of 0.04, and a mean of 0.641, alongside MAPE readings that ranged from a maximum of 84% down to a minimum of 10%, centering at a mean of 38% [41]. Additional performance enhancements have been secured through refinements in the feature selection stage—Minimum Redundancy Maximum Relevance and Minimum Synergy (MRMRMS) serving as a case in point [42]—and through downstream corrective operations, among them Remainder Prediction (RP) [19].

What distinguishes the current contribution is the introduction of a hybridized scheme wherein parametric statistical modeling—exemplified by the Seasonal Autoregressive Integrated Moving Average with Exogenous (SARIMAX) variant—is woven together with machine learning approaches, specifically LSTM and Random Forest (RF). The design draws strength from how these components offset their respective limitations, culminating in a resilient predictive apparatus. The identification of maximally informative predictors proceeds via the tandem deployment of MRMRMS and correlation matrix analysis. Looking ahead to the target horizon, residual magnitudes are forecast and then integrated directly into the concluding prediction, a step that yields a measurable accuracy dividend. The architecture as a whole exploits the capabilities of LSTM, SARIMAX, RF, and Extreme Gradient Boosting (XGBoost), collectively constituting an unprecedented framework for load forecasting.

© 2023 The Author(s). | Published by Institute of Smart Energy Systems Press

Key benefits and novelties of the proposed method:

• Improved accuracy: The statistical machinery accommodates linear associations and cyclical seasonal effects, while the machine learning elements untangle complex nonlinear patterns.

• Reduced overfitting: The statistical side provides an inherent safeguard against overfitting, a property that complements the ML components' ability to navigate complex feature interactions.

• Better feature integration: The assimilation of exogenous variables—meteorological data chief among them—is handled adeptly by the ML stream, all while preserving a lean and stable model structure.

• Dual pattern handling: Responsibility for long-horizon trends and seasonal periodicity rests with the statistical models, leaving short-horizon dynamics and anomalous episodes to be captured by the ML modules.

• Enhanced real-time performance: The agility characteristic of ML, reinforced by the steadiness that statistical methods confer, underpins dependable operation under real-time conditions.

• Improved generalization: Fusing the two modeling philosophies dilutes the weaknesses inherent in each and correspondingly elevates the capacity to generalize.

• Optimized feature selection: The workflow enforces the exclusive retention of salient and mutually non-redundant features, thereby streamlining operations and curtailing noise.

• Reduced computational complexity: Operating on a contracted feature ensemble accelerates runtime execution and strengthens overall computational efficiency.

• Minimized errors: Subjecting the residual series to optimization acts as a brake on error accumulation, with beneficial consequences for predictive fidelity.

Materials and Methods

The point of departure involved compiling and scrutinizing archival consumption time series together with pertinent meteorological readings (encompassing temperature, solar radiation, and dew point). Within the hybrid construct, SARIMAX represents trend trajectories and seasonal regularities, the RF–XGBoost tandem detects nonlinear input-output mappings, and LSTM models temporally conditioned dependencies. The separate outputs from these models are subsequently merged under an ensemble logic, their averaged forecast forming the robust consolidated estimate.

What remains after differencing the predictions from the actual observations—the residual stream—is subjected to diagnostic review, purified via wavelet-domain operations, and carried forward through supplementary analytical apparatus such as the Grey Markov Model to bring structured error dynamics into relief. This bifurcated refinement sequence sharpens the eventual forecast by fusing the preliminary projection with the rectified residual estimate. The overarching methodology is cast to be inherently flexible, readily scalable, and equally applicable to forecasting tasks across both abbreviated and extended temporal spans in the energy sector.

A schematic rendering of the proposed pipeline is furnished in **Figure 2.**

© 2023 The Author(s). | Published by Institute of Smart Energy Systems Press

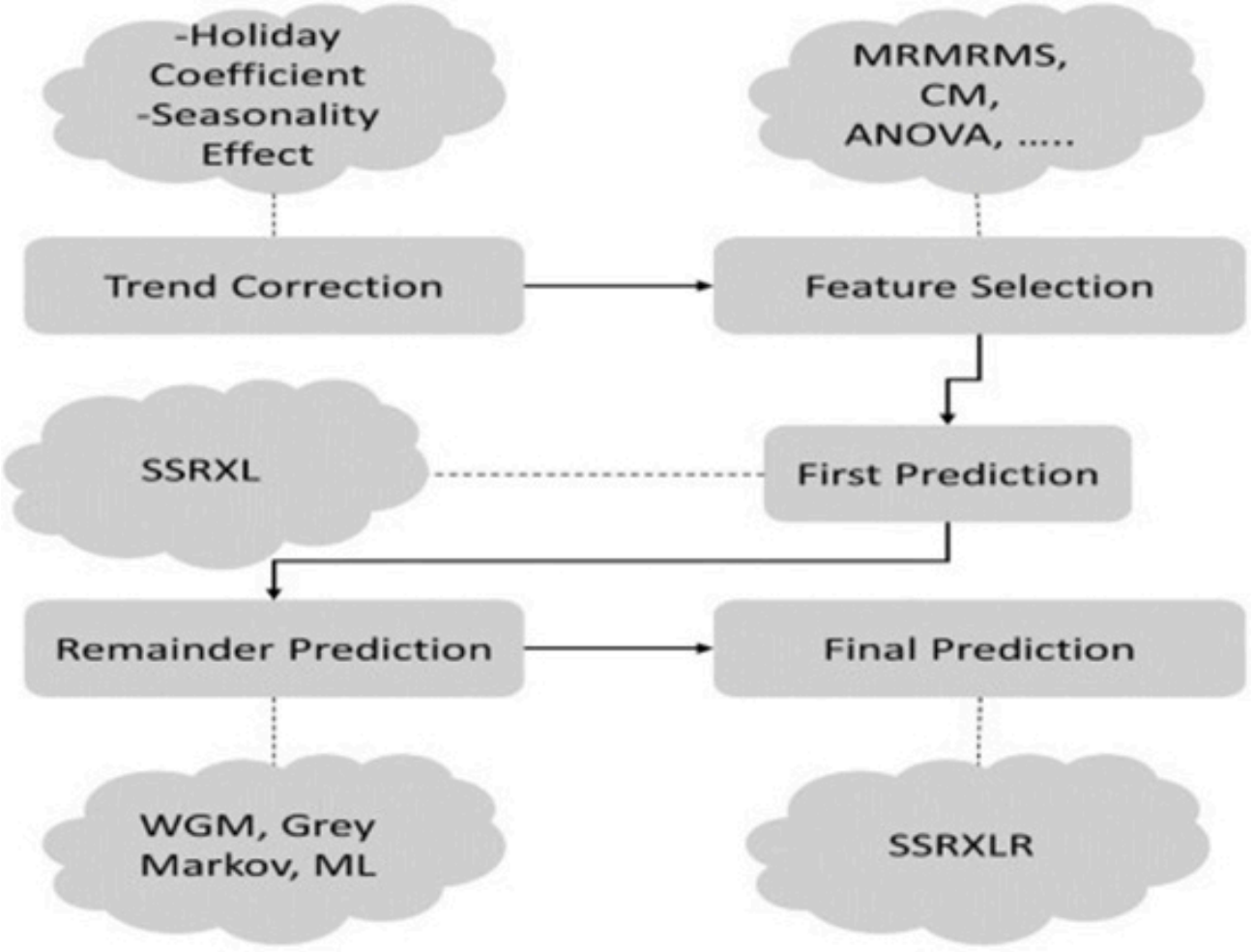

Figure 2. Flow of Procedures of the Proposed Method without Detail about Methods in the First Forecasting Step.

Data description and feature selection

Data description and preparation

The body of data under study consists of electricity consumption observations taken every five minutes across the entirety of the 2022 calendar year, totaling 365 days. These measurements originate from a single residential unit. Recorded in kilowatts (kW), the data trace the electrical demand attributable to the principal domestic appliances, enumerated as follows:

• FAU (Forced Air Unit) Downstairs

• AC (Air Conditioning) Downstairs

• Refrigerator

• AC Upstairs

• General Usage

• Laundry/Dryer

© 2023 The Author(s). | Published by Institute of Smart Energy Systems Press

• Dishwasher/Garbage Disposal

• Microwave

• FAU Upstairs

• Kitchen GFI (Ground Fault Circuit Interrupter)/Toaster

A property that sets this dataset apart is its perfect completeness—absent any missing entries whatsoever—rendering it a thoroughly dependable substrate for investigation. Because the data collection proceeds at a uniform, high-frequency tempo, even granular perturbations in electricity consumption behavior leave a faithful trace; this degree of dependability qualifies the dataset as an exceptional resource for examining the cadences, drifts, and behavioral regularities that define household electricity usage.

Ahead of deploying any predictive models, the dataset is routed through preprocessing and variable screening routines aimed at maximizing downstream model performance. Variable screening serves as a prophylactic against overfitting, and trend adjustment provides a smoothed signal more amenable to accurate forward projection. The 5-minute-resolution consumption profile spanning the full year (2022) for the case-study residence—situated within the Summerlin area of Las Vegas, NV, USA—is portrayed in **Figure 3.**

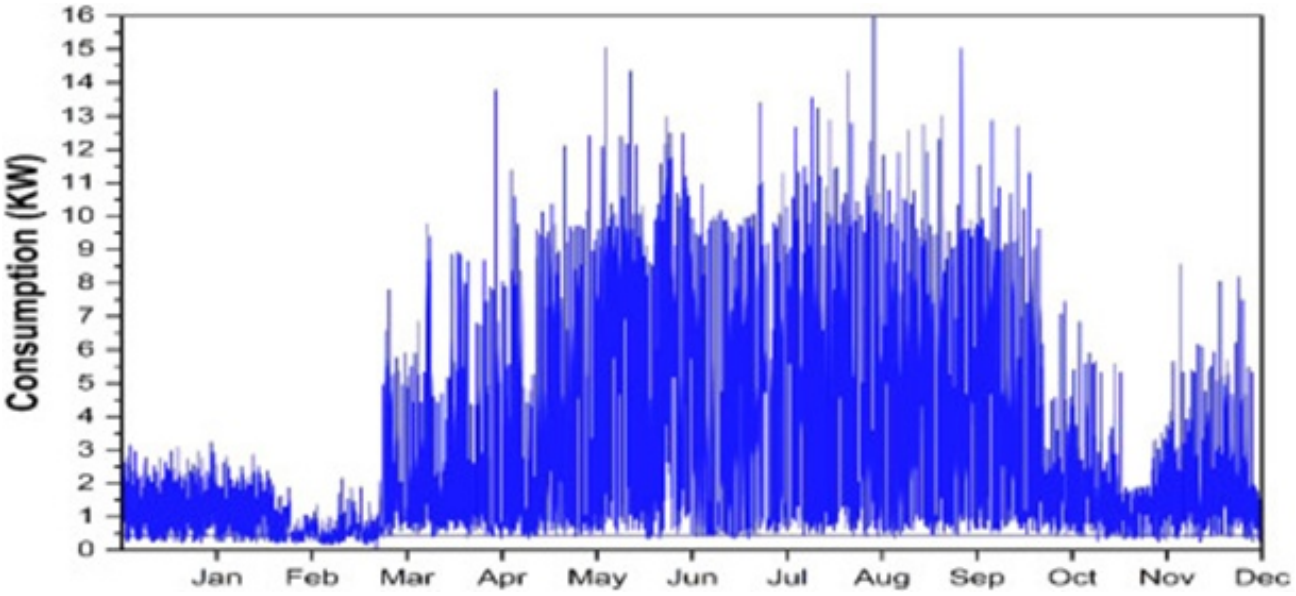

Figure 3. One Year Power Consumption Profile for a Household in Summerlin, Las Vegas.

Modeling the holiday coefficient

The preliminary preprocessing operation entails computing what is termed a holiday coefficient. The rationale is that energy consumption observed on holidays and during weekends injects “noise” into the dataset. Cultural norms, social conventions, and economic pressures can all leave a pronounced imprint on usage during these intervals. To take one example, certain segments of the populace may elect to spend time outside the home, in natural surroundings, or in social gatherings. In contrast, others may choose to remain at home, watching television or receiving guests.

The usage patterns that emerge from these divergent behaviors deviate from conventional weekday profiles and routinely break with seasonal tendencies. Regulatory frameworks likewise exert an influence; manufacturing facilities may operate continuously in some locales, yet stand idle over designated holidays in others.

© 2023 The Author(s). | Published by Institute of Smart Energy Systems Press

Observed Holidays in 2022:

• New Year’s Day: January 1 (Saturday)

• Martin Luther King Jr. Day: January 17 (Monday)

• Presidents’ Day: February 21 (Monday)

• Memorial Day: May 30 (Monday)

• Independence Day: July 4 (Monday)

• Labor Day: September 5 (Monday)

• Columbus Day: October 10 (Monday)

• Veterans Day: November 11 (Friday)

• Thanksgiving Day: November 24 (Thursday)

• Christmas Day: December 25 (Sunday)

The purpose of the Holiday Coefficient is to furnish a quantitative gauge of the degree to which consumption on holidays and weekends parts company with that recorded on standard weekdays. The derivation proceeds along the following chain of operations:

1. Flagging holidays and weekends: A labeling pass over the dataset tags each observation as a holiday, a weekend day, or neither.

2. Categorization: Based on these tags, the data are divided into two strata: holidays/weekends and ordinary weekdays.

3. Average consumption: For each stratum, the arithmetic mean of energy consumption is computed.

4. Coefficient calculation: The holiday coefficient is then formed by taking the ratio of the mean computed for holidays/weekends to the mean computed for regular weekdays.

The arithmetic yields the following set of values:

• Average Consumption on Holidays/Weekends: 1.89 kW

• Average Consumption on Regular Days: 1.94 kW

• Holiday Coefficient: 0.98

The upshot conveyed by this coefficient is that energy usage on holidays and weekends amounts to roughly 97.66 % of the level typical of ordinary weekdays. Embedding this metric within the modeling workflow serves to attenuate spurious variability and, in so doing, sharpens forecasting accuracy.

Modeling the seasonality effect

A uniform month length of 31 days is imposed on every calendar month as the second preprocessing operation. Where a month falls short of 31 days, we pad the record by cloning data points belonging to the concluding day of that month. This

© 2023 The Author(s). | Published by Institute of Smart Energy Systems Press

guarantees dataset-wide consistency, a property that proves indispensable when seasonal rhythms must be analyzed and forecast.

The concept of seasonality captures fluctuations that recur on a predictable schedule—whether daily, weekly, or monthly cycles. Equalizing all months to the 31-day benchmark strips away the confounding influence of unequal month durations and clears the way for the model to extract genuine seasonal signals without distortion.

For the year 2022 under study, this normalization step expands the dataset to a span of 372 days, equivalent to 8,928 hours of observations logged at 5-minute intervals. The resulting compilation holds 107,136 discrete records, a resolution that keeps seasonal signatures intact while supporting fine-grained scrutiny of tendencies on hourly, daily, and monthly scales.

Feature selection

Getting model performance to its peak demands careful feature selection—the act of singling out informative predictors and weeding out duplication. The toolkit commonly brought to bear on this task encompasses the Correlation Matrix (CM), Minimum Redundancy Maximum Relevance (MRMR), ANOVA, the Chi-Square Test, and MRMRMS [4].

Seventeen weather-related variables (itemized below) were downloaded from the Visual Crossing portal [43] for this study; a visual summary appears in **Figure 4** for the geographical setting under investigation.

• Temperature: Degree of atmospheric heat or chill, typically rendered in °C or °F.

• Feels-Like: Perceived thermal sensation synthesizing air temperature, moisture, and airflow.

• Dewpoint: Cooling threshold at which air reaches moisture saturation, reflective of ambient humidity.

• Humidity: Proportion of water vapor suspended in air, quoted as a percentage.

• Precipitation: Aqueous matter—be it rain, snow, sleet, or hail—descending from the atmosphere to the land surface.

• Precipitation probability (PrecipProb): Likelihood of precipitation expressed as a percentage, assisting in meteorological planning and hazard evaluation.

• Snow: Solid precipitation that can affect transport networks, water reserves, and natural habitats.

• Snow depth: Vertical extent of settled snow cover, relevant to mobility, cultivation, and open-air activities.

• Wind gust: Transient spikes in wind velocity, markedly surpassing background sustained speeds.

• Windspeed: Time-smoothed air movement rate, in km/h or mph.

• Wind dir: Bearing from which the wind approaches, stated in degrees clockwise from true north.

• Sea level pressure: Barometric reading adjusted to sea-level equivalent, foundational to synoptic weather analysis.

• Cloud cover: Percentage of the overhead sky obscured by cloud mass.

• Visibility: Maximum unobstructed sighting range for objects or illumination sources.

• Solar radiation: Incoming solar power per unit area, expressed in watts per square meter (W/m^2).

© 2023 The Author(s). | Published by Institute of Smart Energy Systems Press

• Solar energy: Aggregate solar influx accumulated over a stated duration, in kWh/m².

• UV index: Magnitude of ultraviolet radiation exposure.

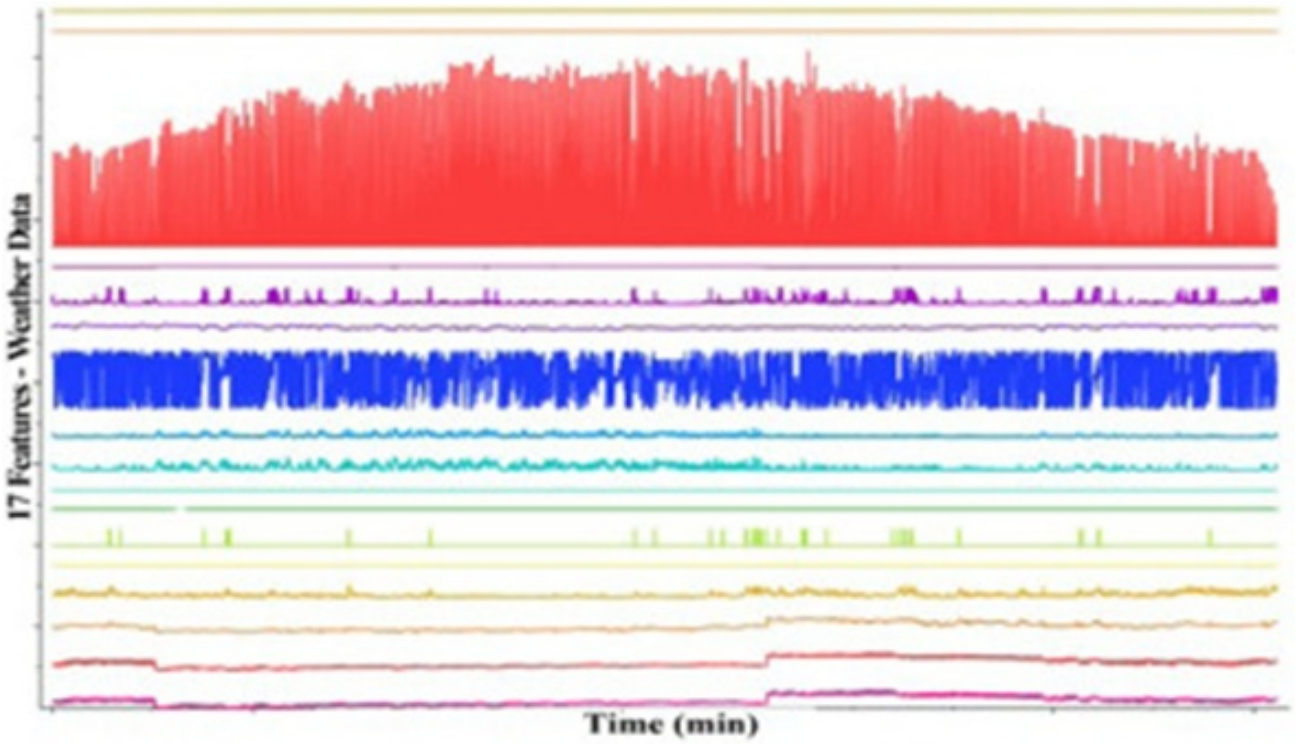

Figure 4. Weather Data for the Location of the Case Study—Household—1-Year 2022 [Summerlin, Las Vegas, NV, USA].

Spotting relationships through naked-eye examination is rendered highly problematic by the dataset's sheer bulk, its erratic fluctuations, and the multitude of driving variables at play.

Time-honored analytical techniques lack the sophistication needed to unravel the intricacies [44] and nonlinear couplings [45] that datasets of this nature harbor. For this reason, Machine Learning (ML) methods are instead harnessed to bring to light underlying configurations [46], inter-variable links [47], convoluted dynamics [48], and directional drifts [49]. Such methods possess the throughput required to digest voluminous data corpora and to surface insights that conventional approaches would leave buried [50].

Correlation matrix

Among the instruments deployed for feature selection, the Correlation Matrix (CM) serves to pinpoint and graphically encode relationships among numerical variables. It operates by evaluating correlation coefficients, which index the strength of linear linkage between variable dyads. Strongly positive coefficients indicate pronounced direct relationships, and strongly negative coefficients indicate powerful inverse connections.

What the CM output conveys, as illustrated in **Figure 5**, is a set of noteworthy associations:

• The most sizable negative linkage with energy consumption is sea level pressure (−0.34), suggesting falling energy use as pressure mounts—a dynamic plausibly mediated by weather-driven shifts in heating and cooling load.

• Robust positive linkages are evident for temperature, feels-like temperature, and dew point (0.32, 0.31, and 0.22, respectively), signaling that warmer and more humid spells drive up energy demand for space cooling.

© 2023 The Author(s). | Published by Institute of Smart Energy Systems Press

• Solar-correlated attributes (UV index, solar radiation, solar energy) present weaker positive ties, centered near 0.17.

• Cloud cover and visibility exhibit virtually no linear association with energy consumption, suggesting their impact is trivial.

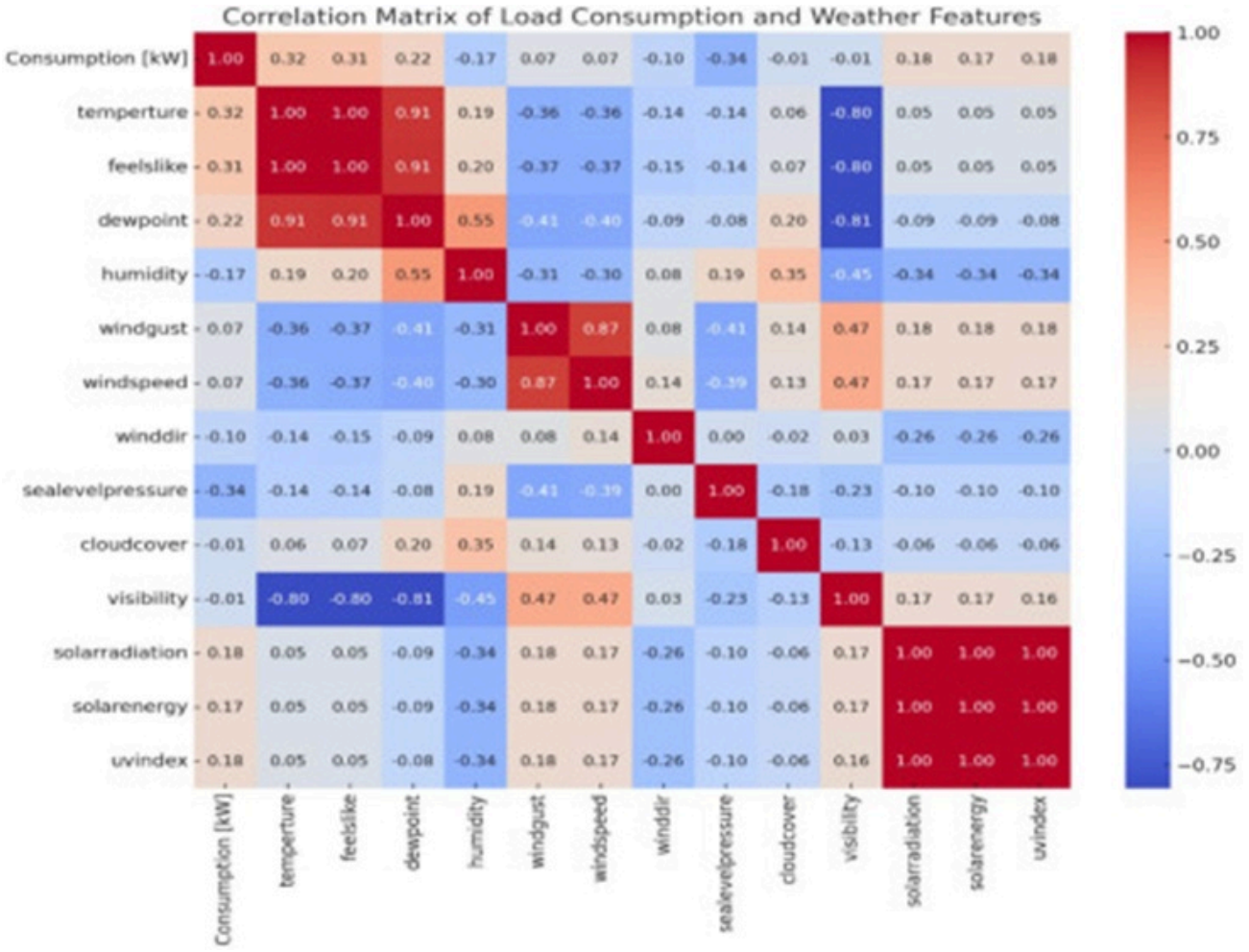

Figure 5. Correlation Matrix Calculated for the 17 Features in **Figure 4**.

Analysis of variance (ANOVA)

The statistical technique termed Analysis of Variance (ANOVA) [51] finds application in feature selection for predictive modeling. Its role is to determine whether individual features register a statistically meaningful effect on the response variable—here, energy consumption. The approach involves contrasting mean consumption values across the tiers of each feature to derive F values (computed as the between-group mean square divided by the within-group mean square). These F values operationalize the ratio of signal across groups to noise within groups, flagging features that carry substantial forecasting weight.

The resulting picture, laid out in **Figure 6**, warrants the following observations:

• At the top of the predictor hierarchy sits sea level pressure, with temperature occupying the runner-up position.

© 2023 The Author(s). | Published by Institute of Smart Energy Systems Press

• Solar-aligned quantities (solar radiation, solar energy, and UV index) are shown to exert a meaningful pull on energy usage.

• Both dew point and humidity likewise register as significantly influential.

• The F values for visibility and cloud cover are markedly lower, suggesting negligible bearing.

• Wind-linked measures (wind speed and wind gusts) produce subdued readings, their influence paling relative to thermal and solar factors.

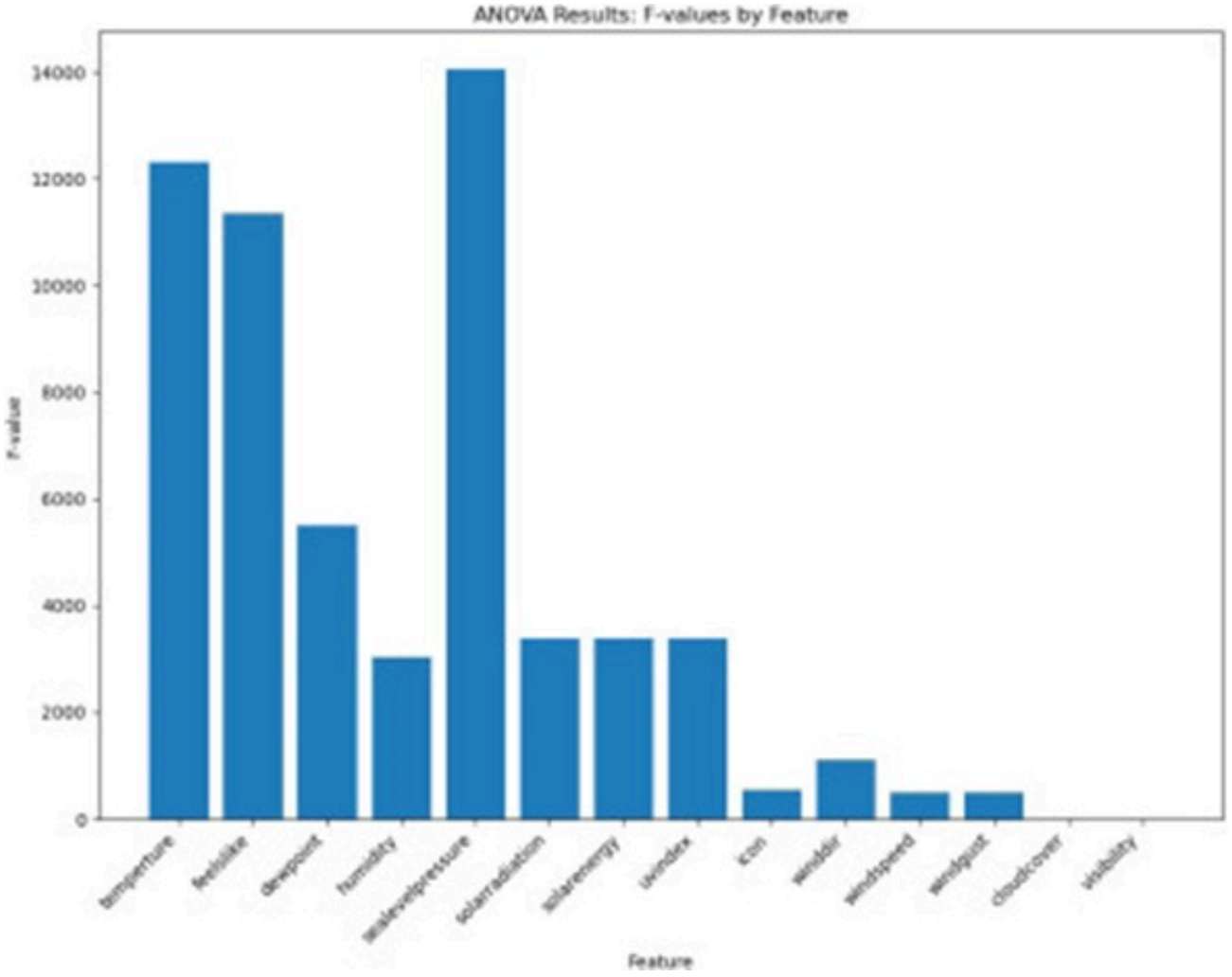

Figure 6. Calculated F-Values (ANOVA).

A clear implication emerges from these outcomes: variables such as sea level pressure, temperature, apparent temperature, and dew point carry the greatest weight in projecting energy consumption. Features of marginal relevance—visibility and cloud cover among them—might justifiably be dropped, thereby tightening model parsimony and boosting predictive throughput.

Minimum redundancy maximum relevance and minimum synergy (MRMRMS)

The MRMRMS algorithm is a feature selection strategy engineered to raise predictive accuracy by negotiating a trade-off between individual feature relevance and collective redundancy. Its evaluative currency is mutual information—a measure that quantifies the reduction in uncertainty about one variable after learning about another. Features that simultaneously

© 2023 The Author(s). | Published by Institute of Smart Energy Systems Press

post high relevance to the target (energy consumption) and low mutual overlap are the ones the method retains, guaranteeing that each contributes distinctive informational content.

Operationally, MRMRMS begins with standardizing the dataset's numeric columns, after which mutual information values are calculated for each candidate feature. The standardization transformation recasts every variable such that its distribution is centered at zero with unit dispersion. It is expressed through the formula:

$$StdV = \frac{V - \mu(V)}{\sigma(V)} \quad (1)$$

Where StdV represents the post-transformation value, V is the untransformed observation, μ denotes the arithmetic mean of V, and σ its standard deviation. This preprocessing step neutralizes the distorting potential of incommensurate scales and measurement units.

Mutual information scores encapsulate how much predictive leverage each feature supplies with respect to energy consumption. Ranking by these scores brings forward features that marry high informational relevance with low inter-feature redundancy.

A distinction worth underlining: standardization does not, as normalization does, confine data within a bounded interval (such as 0 to 1) and refrains from presuming any particular distributional geometry. This renders it the method of choice for algorithms that assume Gaussian-distributed inputs. The MRMRMS outcomes are tabulated in **Table 1**, where temperature and feels-like temperature stand revealed as the premier influences on energy consumption—testimony to the dominance of thermal drivers. Moderate influence is attributable to dew point, sea level pressure, and humidity. At the lower bound, solar energy and visibility betray comparatively faint relevance to patterns of energy use.

Table 1. Score of MRMRMS Features.

Feature	Solar Radiation	Solar Energy	Sea Level Pressure	UV Index	Feels-Like	Temperature
Score	0.153	0.073	0.203	0.052	0.381	0.386
Feature	Cloud cover	Wind gust	Wind speed	Wind dir	Humidity	Dew point
Score	0.085	0.114	0.106	0.139	0.159	0.242
Feature						Visibility
Score						0.040

The interpretation that flows from these results is that energy consumption pivots mainly on temperature-anchored variables, which act directly on heating and cooling loads. Meteorological phenomena such as solar energy and visibility play a less central role, diminishing their importance within predictive modeling constructs.

Chi-Square test

Assessing the independence of categorical variables is the domain of the Chi-Square Test [52]. Transplanted into the load forecasting context, this test quantifies the tightness of association linking discretized atmospheric features with binned consumption categories. A large chi-square statistic indicates a strong association between a feature and energy usage, making it a salient predictor.

© 2023 The Author(s). | Published by Institute of Smart Energy Systems Press

Putting the Chi-Square Test into practice calls for dividing continuous meteorological readings into discrete strata and for grouping load consumption values into bins or ranges. The procedure yields a Chi-Square statistic that formalizes the mismatch between empirically observed frequencies and those anticipated under an assumption of independence. In this manner, weather variables that are critically linked to load consumption are identified and ordered by their statistical weight.

The synthesis displayed in **Table 2** points to temperature, feels-like temperature, UV index, sea level pressure, solar energy, and solar radiation as the meteorological determinants most tightly coupled with energy consumption. These variables predominantly shape energy usage routed through heating, air conditioning, and solar energy systems. Dew point and humidity occupy an intermediate tier in terms of influence, while visibility and cloud cover trail behind, their associations too faint to carry meaningful predictive weight.

Table 2. Scores of Chi-Square Test.

Feature	Solar Radiation	Solar Energy	Sea level pressure	UV index	Feels-Like	Temperature
Score	4151.809	4176.774	4775.704	4932.46	5907.64	7162.332
Feature	Cloud cover	Wind gust	Wind speed	Wind dir	Humidity	Dew point
Score	284.650	600.80606	676.616	867.17	2270.17	3776.295
Feature						Visibility
Score						55.890

Statistical significance was confirmed for every variable examined, as evidenced by p-values (understood as the probability of observing a test statistic equal to or more extreme than the one obtained, given the validity of the null hypothesis) that fell below conventional thresholds. This result corroborates their collective relevance within the load forecasting domain. That the analytical lens ought to be trained principally on the most discriminating predictors—temperature, feels-like temperature, and solar-correlated quantities—while backgrounding features of lesser consequence such as visibility and cloud cover is a central implication of these outcomes. Models of greater efficiency and parsimony become attainable when construction efforts are concentrated on those inputs exhibiting the strongest empirical linkage with energy draw.

The uppermost features flagged by each selection methodology are enumerated as follows:

• CM: Sea level pressure, temperature, feels-like temperature, and dew point.

• ANOVA: Sea level pressure, temperature, feels-like temperature, and dew point.

• MRMRMS: Temperature, feels-like temperature, dew point, and sea level pressure.

• Chi-square: Temperature, feels-like temperature, UV index, and sea level pressure.

Across every technique applied, a consistent triumvirate of sea level pressure, temperature, and feels-like temperature occupies the topmost ranks, trailed in the fourth slot by dew point. On this basis, the quartet of features designated for retention consists of:

• Sea level pressure

© 2023 The Author(s). | Published by Institute of Smart Energy Systems Press

• Temperature

• Feels-like

• Dew point

Proposed load forecasting method

Within the methodology advanced here, state-of-the-art machine learning algorithms and statistical models are interlaced into a unified pipeline geared toward delivering high-fidelity energy load projections together with RP. At the front end of the workflow lies the gathering of relevant data streams—archival consumption time series and meteorological covariates encompassing temperature, sea level pressure, dew point, and solar radiation. Motivated by their established bearing on patterns of energy utilization, these candidate predictors undergo deliberate curation, a winnowing process that heightens the precision attainable by the downstream forecasting apparatus.

An ensemble design philosophy lies at the architectural heart of the methodology: four separate modeling formalisms are marshaled—Random Forest (RF), Long Short-Term Memory (LSTM), Seasonal Autoregressive Integrated Moving Average with Exogenous Variables (SARIMAX), and Extreme Gradient Boosting (XGBoost). Training proceeds independently for each, to capture a distinct dimension of the predictive challenge. Temporal trajectories and seasonal periodicities embedded within the consumption chronicle constitute the analytic territory of SARIMAX. The charge of RF and XGBoost, conversely, is to map the nonlinear pathways through which meteorological drivers translate into energy demand. LSTM, engineered from the ground up for ordered sequential data, lays hold of lagged temporal contingencies spanning both the consumption and atmospheric variable streams. The separate model outputs are fused through simple arithmetic averaging, producing a consensus ensemble forecast. This tactic reconciles the unique strengths residing in each constituent and correspondingly raises the composite predictive standard.

A secondary phase is activated once the preliminary load forecast has been generated; its objective is to address the residual mismatches between predicted and realized figures. Subtracting the ensemble forecast from the ground-truth consumption chronology quantifies this deviation. Diagnostic examination of the resultant error series is undertaken to isolate any systematic bias and project the adjustments required to offset it. The selfsame ensemble of models and features is enlisted to predict these corrective quantities, a procedure that effectively constitutes a “remainder forecast.” The conclusive energy consumption estimate is then constructed by adding the projected deviation onto the initial ensemble forecast. This two-tiered architecture ensures that macro-scale consumption movements and micro-level departures alike receive due consideration, thereby substantially reinforcing the credibility of the final forecast.

Empirical substantiation of the methodology is secured by measuring the finalized predictions against actual consumption records, using both numerical yardsticks—Mean Absolute Error (MAE) and Root Mean Squared Error (RMSE)—and side-by-side graphical inspection. By combining disparate modeling traditions and embedding an error-correction feedback loop, the scheme described here furnishes a hardened, precise energy load forecasting capability, sensitively tuned to the shifting contours of actual consumption behavior.

This methodology confers a constellation of significant advantages: Marrying a statistical workhorse such as SARIMAX with machine learning counterparts—RF, XGBoost, and LSTM—empowers the framework to apprehend temporally governed regularities and nonlinear input-output relationships in equal measure, yielding forecasts of elevated accuracy. The capacity to account for exogenous atmospheric forcing is secured through the inclusion of weather-side variables, lending predictive dependability across a spectrum of environmental regimes. The ensemble construction hedges against the twin hazards of overfitting and underfitting by balancing the respective contributions of each model, while the dual-phase structure incorporating RP takes direct aim at residual error, enabling finer-grained adjustment.

© 2023 The Author(s). | Published by Institute of Smart Energy Systems Press

Additionally, flexibility and scalability are baked into the methodological design from the outset, enabling reconfiguration for heterogeneous datasets and divergent forecast windows—a property of considerable practical value within live energy management deployments. The singular synthesis of modeling modalities and corrective stages not only amplifies predictive exactitude but also deepens robustness and agility in the face of evolving consumption profiles. As a result, the method represents a well-calibrated response to the stringent requirements of trustworthy energy forecasting over both near-term and distant timeframes. A diagrammatic exposition of the procedural sequence is provided in **Figure 7**, while implementation particulars are unpacked across **Figures 8 through 10.**

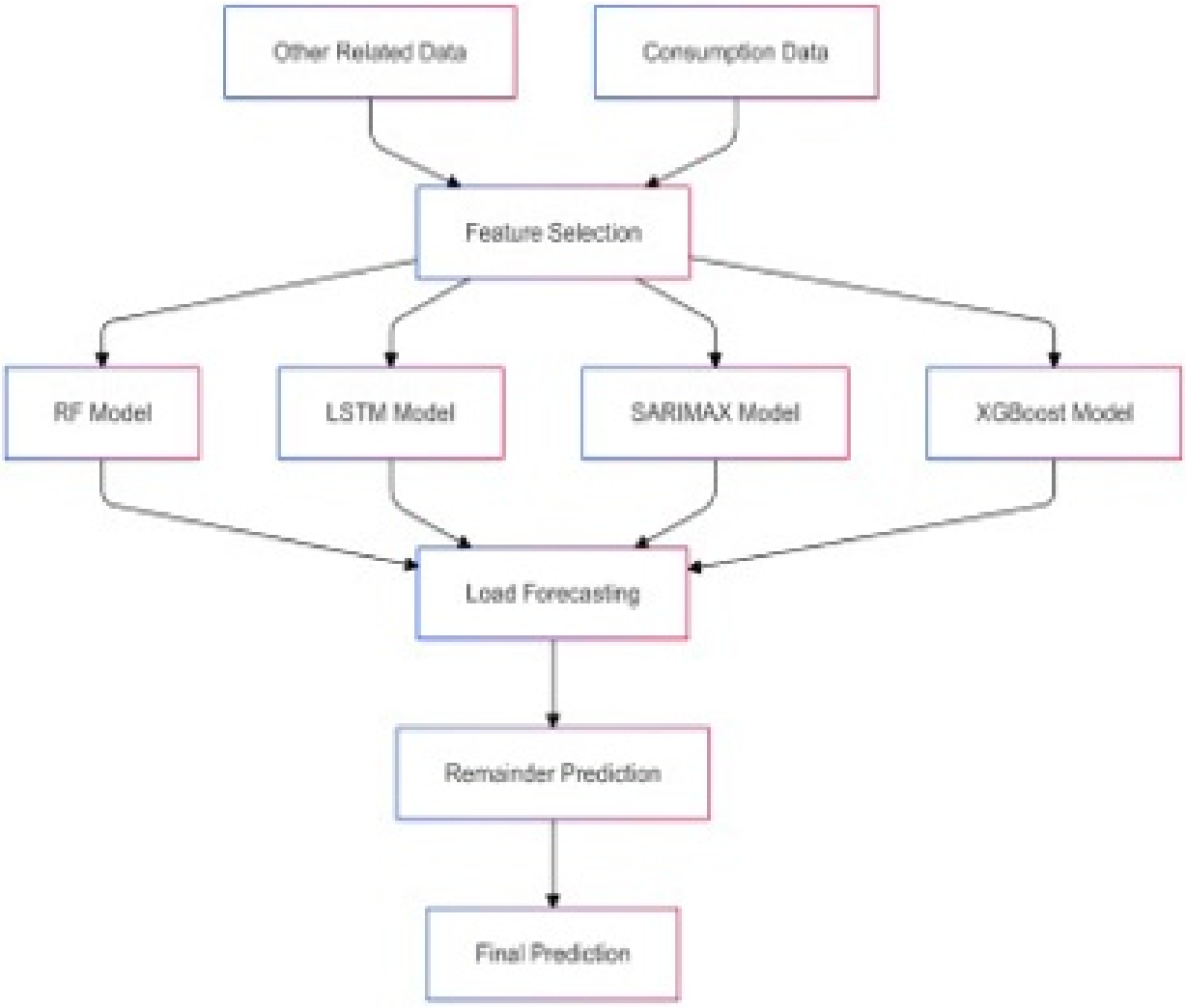

Figure 7. SSRXLR: Flow of Procedures.

© 2023 The Author(s). | Published by Institute of Smart Energy Systems Press

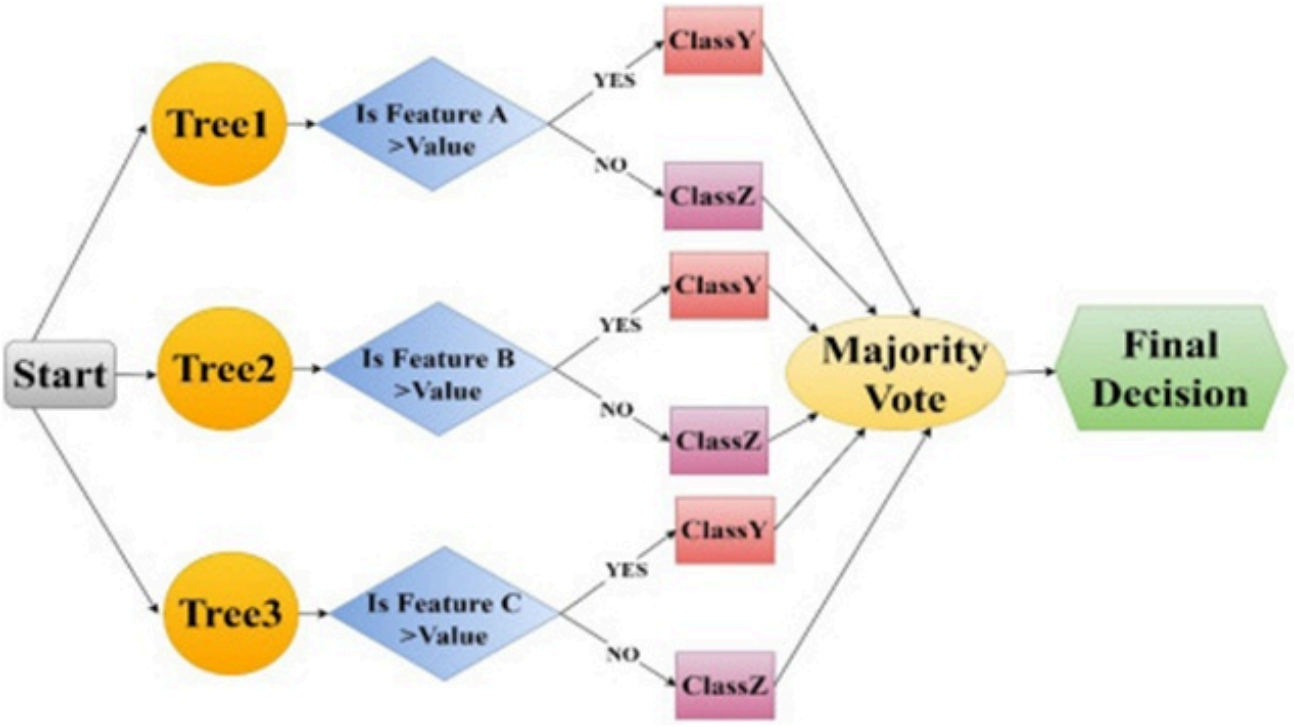

Figure 8. Random Forest Model.

Random forest

What **Figure 8** presents is the Random Forest model—an ensemble learning strategy whose robustness derives from multiplying simple decision trees far beyond a single tree's capacity, all in service of elevated predictive performance. Rather than relying on any one tree, the collective renders its verdict by aggregating individual tree outputs: votes are tallied for classification, and numerical predictions are averaged for regression problems. The architecture that results from this design is well-balanced, possessing the wherewithal to manage noisy measurements, outlying data points, and gaps in the record without breaking down.

Few algorithms match the sheer versatility that Random Forest brings to bear. One particularly prized capability is its aptitude for ordering features by their contribution to predictive success—a property that makes it an essential asset during the variable selection phase and for probing the inner logic of the trained model. Where structured data are involved, Random Forest habitually turns in strong showings, a track record spanning domains as far-flung as banking fraud screening, grid-level load projection, clinical diagnostic classification, e-commerce product recommendation, and taxonomic assignment in the life sciences.

These advantages are, however, purchased at a certain price. The very ensemble nature that gives Random Forest its power simultaneously drives up the computational budget and the memory footprint required. When the model harbors numerous deep-grown trees, the time needed to return a prediction can become appreciable. An additional trade-off concerns interpretability: unlike a solitary decision tree, whose logic can be traced directly, the aggregated Random Forest resists straightforward explanation, remaining considerably more inscrutable.

Yet for all these qualifications, Random Forest has lost none of its standing as a widely embraced and trustworthy algorithm. The combination of forceful generalization, tolerance for diverse data modalities, and built-in defenses against overfitting ensures it remains the go-to option across a broad landscape of applications where getting the prediction right, and doing so dependably, is the overriding concern.

© 2023 The Author(s). | Published by Institute of Smart Energy Systems Press

Extreme gradient boosting

Figure 9 provides a schematic view of Extreme Gradient Boosting (XGBoost), a machine learning framework distinguished by its suppleness and computational economy, engineered for supervised problem settings that span regression, classification, and ranking. The niche occupied by time-series-dedicated statistical machinery—ARIMA and SARIMAX being representative specimens—is quite distinct from the expansive terrain that XGBoost inhabits, a terrain in which structured data of virtually any stripe, temporal sequences among them, can be tackled once the problem is suitably recast under a supervised learning rubric. The superlative performance for which XGBoost is known flows from its sequential tree-building logic: each successive tree is optimized to counteract the mistakes that its predecessors left behind. Salient strengths include sheer computational throughput, exactitude of fit, and operational adaptability. Native affordances encompass user-specified loss formulations, graceful absorption of missing entries, and embedded regularization penalties that act as bulwarks against overfitting.

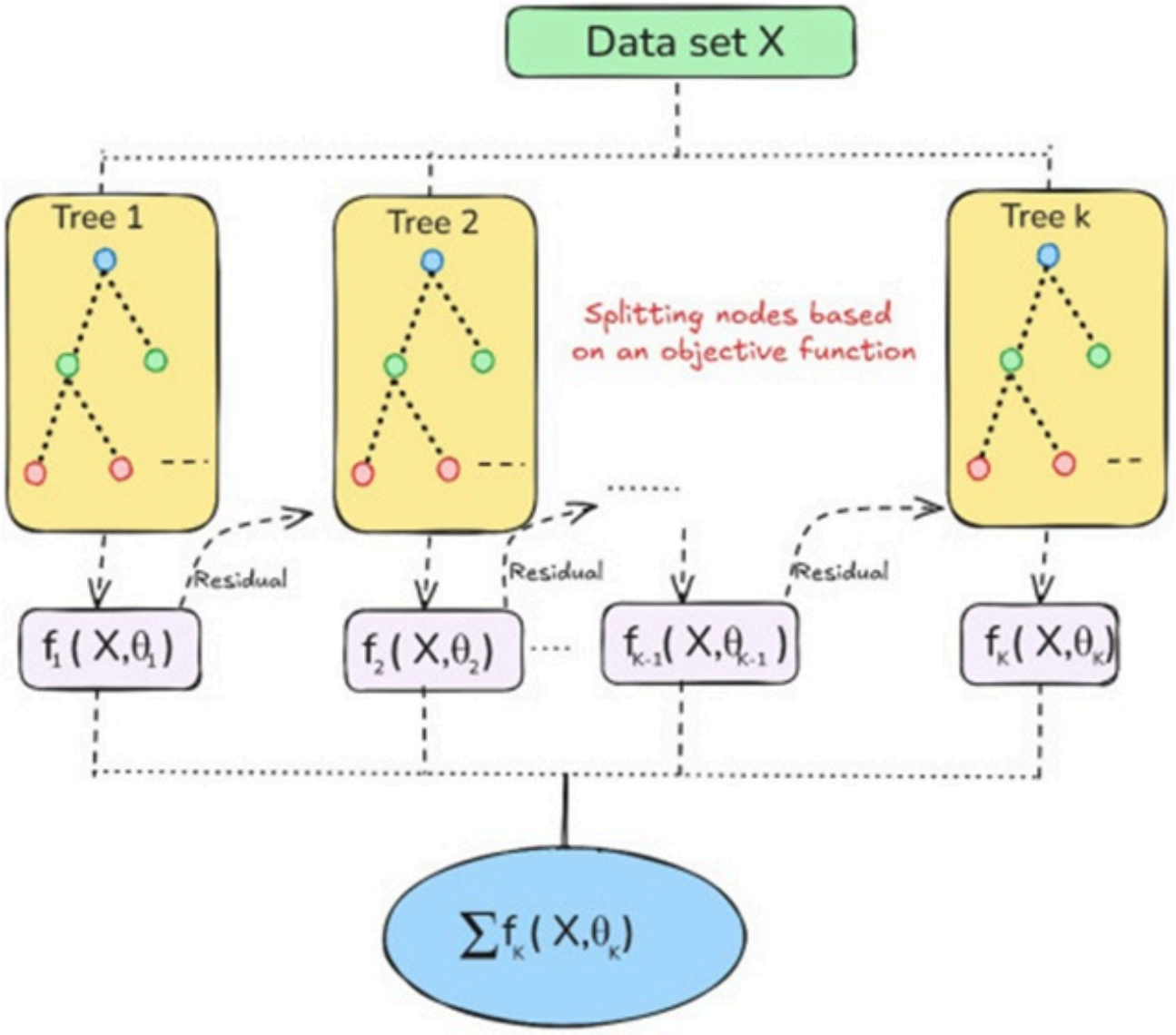

Figure 9. Architecture of XGBoost.

Though time series forecasting does not belong to XGBoost's original design brief, the algorithm can be productively redirected toward such ends when coupled with judiciously engineered inputs. The preparatory work customarily involves constructing lagged copies of target and predictor series, computing moving-window aggregates, and appending

© 2023 The Author(s). | Published by Institute of Smart Energy Systems Press

calendar-derived markers—day-of-week, month-of-year, or seasonality flags being typical examples. Preservation of temporal ordering during the division into training and holdout partitions is assured through disciplined protocols, rolling-window expansion foremost among them. What sets XGBoost apart in the time series arena is its facility for modeling nonlinear mappings and for absorbing exogenous covariates, twin strengths that render it particularly well-matched to complex, nonlinear temporal datasets.

Certain limitations do attend the XGBoost framework. A heavy reliance on manually sculpted features translates into a time investment that presupposes familiarity with the application domain. In multi-step recursive forecasting configurations, the compounding of errors across successive prediction horizons is a further concern, since each forward step relies on previously estimated values. Yet even with these caveats, XGBoost stands as a formidable alternative—or companion—to the classical statistical toolkit, above all when the data under study are high-dimensional, densely multivariate, or exhibit non-stationary behavior.

Long short-term memory (LSTM) networks

Long Short-Term Memory (LSTM) networks, their generic structural blueprint shown in **Figure 10**, occupy a specialized branch of the Recurrent Neural Network (RNN) family tree, expressly devised to overcome a well-known shortcoming of standard RNNs: their struggle to capture dependencies that stretch across long intervals within ordered data. The pathology that cripples conventional RNNs—vanishing gradients, whereby the backpropagated signal attenuates to a level too feeble to drive meaningful weight adaptation—is effectively cured by the LSTM formulation. The pivotal innovation is a memory cell structure that can safeguard information across extended temporal spans, conferring on LSTMs an exceptional aptitude for tasks where context must be carried forward over many time steps, temporal forecasting, speech-to-text conversion, and natural language processing (NLP) being prominent exemplars.

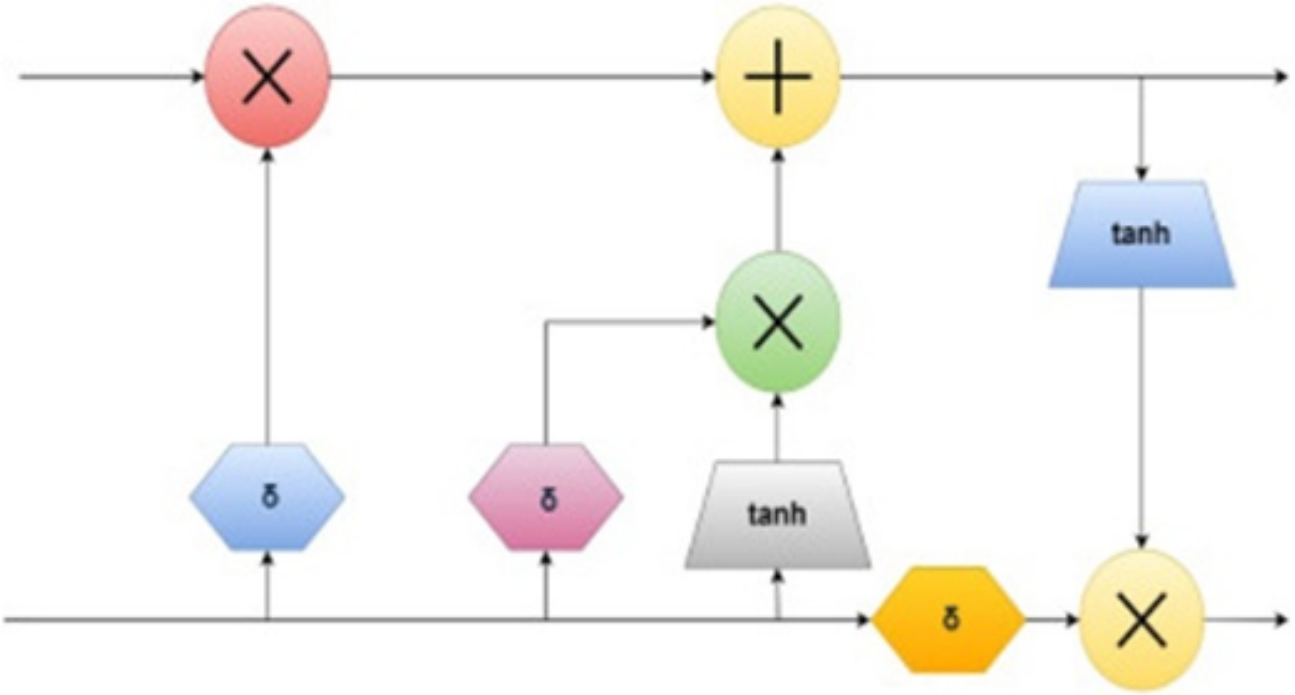

Figure 10. LSTM Model.

At the functional core of the LSTM lie three gating units—designated forget, input, and output—whose coordinated operation determines, instant by instant, which information is retained intact within the memory cell, which is modified,

© 2023 The Author(s). | Published by Institute of Smart Energy Systems Press

and which is expunged. This tripartite regulatory scheme achieves a carefully tuned compromise between sensitivity to transient signals and fidelity to long-run structure, a balance that confers on LSTMs their singular fit with sequential data-processing challenges.

The imprint of LSTMs on multiple fields of application is unmistakable. Within NLP, they have propelled advances in statistical language modeling, automated text generation, and interlingual machine translation, leveraging their capacity to encode the surrounding linguistic context and to anticipate structured sequential outputs. The speech recognition community has drawn on LSTMs to decompose temporally extended acoustic waveforms into transcribed verbal content with a high degree of fidelity. Anomaly detection represents yet another domain of utility, with LSTMs deployed to isolate unusual segments in streaming time series.

LSTMs are not without their burdens. Architectural intricacy and dense parameterization combine to produce a heavy computational appetite, while the stepwise, time-locked nature of their operation places inherent limits on parallelizability—a contrast with alternative architectures such as Convolutional Neural Networks (CNNs) that is particularly stark. These impediments notwithstanding, the flexibility of LSTMs—their equal readiness to consume solitary data vectors or entire sequences—has firmly entrenched them as foundational infrastructure within the deep learning ecosystem. It is this very adaptability that continues to catalyze progress in the representation and analysis of data unfolding through time.

Seasonal autoregressive integrated moving average with exogenous variables (SARIMAX)

A step up in sophistication from the baseline ARIMA framework, SARIMAX functions as a time series forecasting instrument expressly tailored for data shaped by two concurrent phenomena: periodic oscillations that resurface at predictable intervals (be they monthly or annual cycles) and the pull of exogenous variables—outside forces that leave a detectable mark on the target series. SARIMAX achieves this by uniting three analytical capabilities under one roof: the seasonal modeling machinery of SARIMA, the non-seasonal trend apparatus of ARIMA, and the capacity to fold in auxiliary predictors that elevate forecasting fidelity. Written generically, the model specification is:

SARIMAX (p, d, q)(P, D, Q)[s] + X

The specification integrates three distinct building blocks:

• 2022 Non-seasonal elements – encoded by the triple (p, d, q), which together capture autoregressive behavior, the degree of differencing applied, and the moving average structure.

• Seasonal elements – encoded by (P, D, Q)[s], which jointly represent the cyclic regularities woven through the data.

• Exogenous variables (X) – supplemental external covariates that bear upon the series of interest.

1) ARIMA Component (non-seasonal part):

$$\phi(\mathrm{B})\ (1-B)^{d} yt\ = \theta(\mathrm{B})\ \epsilon_t \quad (2)$$

Where:

• ϕ(B): Non-seasonal autoregressive (AR) polynomial of order p.

• θ(B): Non-seasonal moving average (MA) polynomial of order q.

• B: Backward shift operator

© 2023 The Author(s). | Published by Institute of Smart Energy Systems Press

• d: Number of non-seasonal differences.

• y_t: The target variable at time t.

• ϵ_t: White noise error term.

2) Seasonal Component:

$$\Phi(B^s)(1-B^s)^D yt = \Theta(B^s)\,\epsilon_t \quad (3)$$

Where:

• $\Phi(B^s)$: Seasonal autoregressive polynomial of order P.

• $\Theta(B^s)$: Seasonal moving average polynomial of order Q.

• S: Seasonality period

• D: Number of seasonal differences.

3) Exogenous variables (X):

$$yt = \beta X_t + \epsilon_t \quad (4)$$

• Xt: External (exogenous) regressors at time t.

• β: Coefficient vector for the exogenous variables.

Bringing all pieces together, the composite SARIMAX formulation can be written as:

$$\phi(B)(1-B)^d\Phi(B^s)(1-B^s)^D y_t = \theta(B)\Theta(B^s)\epsilon_t + \beta \quad X_t \quad (5)$$

This construction yields a model equipped to handle dependency structures operating on both non-seasonal and seasonal timescales, to deploy differencing as a stationarity-inducing transformation, and to incorporate outside influences through external covariate terms formally.

This architectural flexibility positions SARIMAX as a formidable and adaptable instrument across a diverse array of practical settings—from projecting merchandise sales that follow seasonal rhythms to forecasting electrical load in response to atmospheric drivers to modeling any temporal process known to be sensitive to external stimuli. Its dual capacity to represent seasonal dynamics and to register the effect of exogenous variables enables SARIMAX to deliver forecasts that combine sharpness with explanatory insight, even when the underlying scenario is far from simple.

SSRXLR

A pseudocode rendering of the SSRXLR algorithm proposed in this work is supplied below **(Algorithm 1)**:

© 2023 The Author(s). | Published by Institute of Smart Energy Systems Press

Input: *Historical load data, Weather features, Forecast horizon* = *12* Step 1: Data Preprocessing
Normalize data using MinMaxScaler to range [0, 1]
Step 2: Feature Selection
Select relevant features (historical load, temperature, etc.)
Step 3: Model Training and Prediction
Train SARIMAX model with seasonal and non-seasonal components
Predict next 12 points → SARIMAX_Output
Train RF model using weather and historical data
Predict next 12 points → RF_Output
Train XGBoost model using weather and historical data
Predict next 12 points → XGBoost_Output
Train LSTM model for time-series forecasting
Predict next 12 points → LSTM_Output
Step 4: Ensemble Averaging
Ensemble_Output = (SARIMAX_Output + RF_Output + XGBoost_Output + LSTM_Output) / 4
Step 5: RP
Perform additional adjustments if needed
Step 6: Output Final Prediction
Return Ensemble_Output

Algorithm 1. Pseudocode of the Proposed Algorithm.

The rationale for operating an ensemble of models extends beyond the mere pursuit of heightened accuracy; the practice also yields a more rounded analytical view, since it synthesizes disparate modeling philosophies, each injecting its own distinctive signal into the composite forecast. **Table 3** reports the projections cast by the proposed method across the next 12 temporal intervals. The gaps separating projected from actual readings can be ascribed to a shortfall in available predictor coverage—specifically, the dataset lacks variables capturing the psychological disposition and habitual routines of household occupants, the size of the resident population, household economic standing, and episodic yet significant happenings such as birthdays and wedding anniversaries.

Table 3. Predicted consumption (KW) for next points by proposed method before applying RP.

Point	12	11	10	9	8	7	6	5	4	3	2	1
Actual	0.669	0.989	1.732	0.664	0.625	0.59	0.56	0.846	1.84	0.752	0.646	0.65
SSRXL	0.884	0.958	1.036	0.87	0.876	0.879	0.883	0.972	1.064	0.864	0.867	0.874

To bridge the gap left by these missing predictors, the RP step is activated as described next. This step first involves diagnosing the trend embedded within the residual stream and subsequently projecting residual magnitudes forward across 12 steps. The final estimate of consumption is then arrived at by layering these projected residuals on top of the initial forecasted consumption figures.

Modeling of the remainder prediction

Remainder prediction plays a key role in forecasting workflows: pinpointing and adjusting the departures—termed residuals—that arise between projected figures and their actual counterparts [53]. The ongoing accuracy and

© 2023 The Author(s). | Published by Institute of Smart Energy Systems Press

dependability of predictive models hinge critically on these adjustments, a truth that becomes especially acute in dynamic regimes where even marginal errors can snowball across successive time horizons.

Systematic biases can be held in check, aggregate accuracy elevated, and responsiveness to unforeseen data shifts sharpened when the remainder itself is the object of careful forecasting. The pertinence of this practice intensifies in settings where decisions are time-critical and the ability to update forecasts in close to real time can materially sway operational choices. The RP landscape accommodates several alternative methodologies. A synopsis of three especially prevalent options is furnished in **Table 4**, with each contributing a unique angle on residual characterization and on the reinforcement of forecasting reliability as circumstances vary [54-56].

Table 4. Comparison of different methods for RP.

Model	Key features	Strengths	Challenges
Wavelet Residual Modified Grey Forecasting Model (WGM) [54]	• Applies wavelet transforms to model residual components• Uses wavelet basis functions for error adjustment• Improves handling of nonlinear forecasting patterns	• Enhances prediction accuracy for nonlinear time-series data• Provides effective residual error correction	• Selecting appropriate wavelet basis functions is complex• High computational cost when applied to large datasets
Grey Markov Model [55]	• Integrates Grey forecasting with Markov chain modeling• Performs residual state transition analysis• Based on a probabilistic state-transition framework	• Strong performance in state-dependent systems• Improves accuracy via residual correction using state transitions	• Requires sufficient historical state data for reliable Markov modeling• Performs poorly in highly dynamic or rapidly changing systems
Residual Correction in Real-Time Traffic Forecasting (ResCAL) [56]	• Model-agnostic residual correction framework• Uses autocorrelation properties of residuals• Incorporates graph signal processing for traffic error adjustment	• Enables real-time residual estimation• Can be applied across different forecasting models to improve traffic prediction	• Real-time accuracy may degrade due to data latency• Highly dependent on the quality of historical residual data

The contribution of the present work includes an original RP methodology (**Figure 11**) that interlaces statistical modeling, machine learning, and the tools of signal processing to hone predictive precision and to offset systematic deviations. At the front of the pipeline sits the Discrete Wavelet Transform (DWT), to which the residual series—obtained by subtracting forecasted values from actual observations—is fed. DWT resolves this series into a low-frequency band (approximation coefficients, within which broader trends are encoded) and a high-frequency band (detail coefficients, where noise and sharp discontinuities reside). High-pass filtration isolates and discards the noise component, while low-pass filtration retains the structurally coherent signal. The net effect of this wavelet-based processing is a marked suppression of high-frequency contamination, accompanied by the preservation of low-frequency trend content; the outcome is a cleaner, information-richer input for downstream analytical stages.

© 2023 The Author(s). | Published by Institute of Smart Energy Systems Press

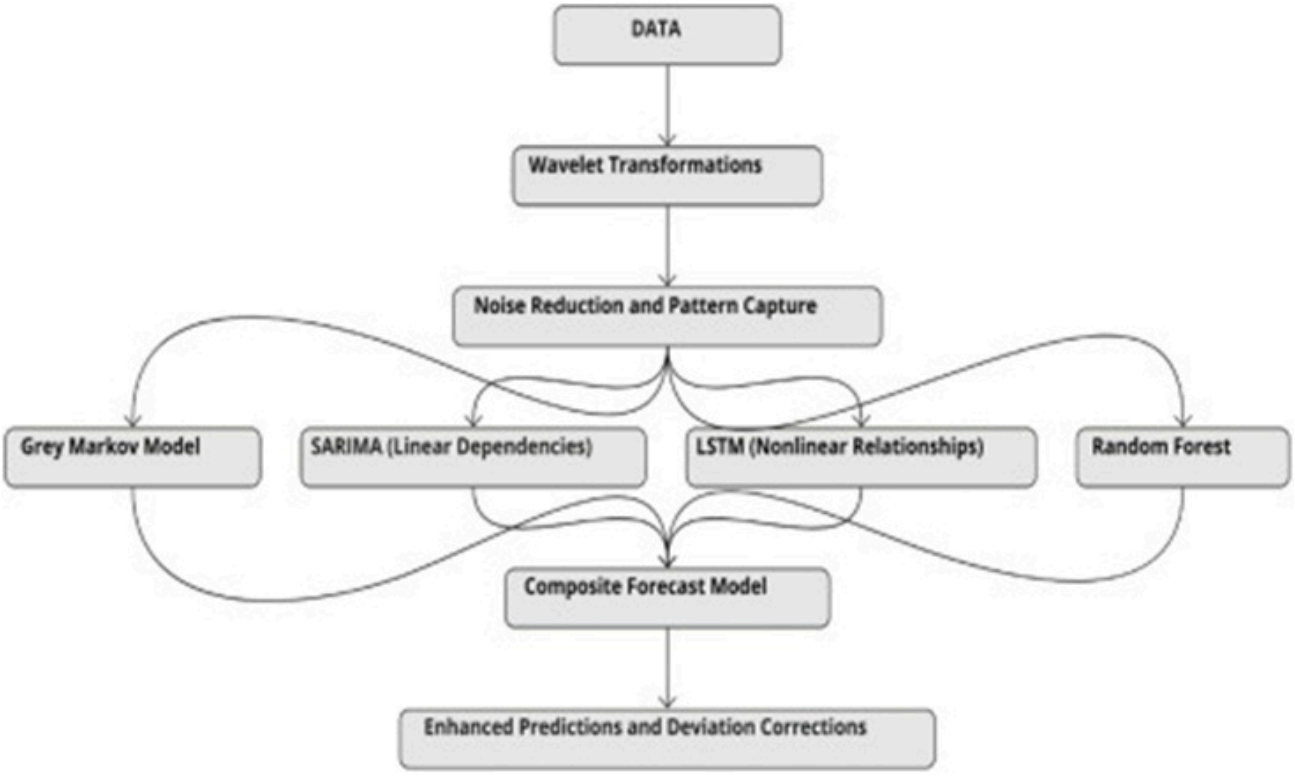

Figure 11. Remainder Prediction Algorithm.

With preprocessing concluded, the residual sequence is handed over to the Grey Markov Model for diagnostic scrutiny. This model segments the residuals into a collection of discrete states and applies Markov chain formalism to the probabilistic transitions linking one state to the next. The resulting state-conditioned framework allows predictions to be continuously re-anchored to the latest observed trends, conferring the nimbleness to react swiftly when incoming data shift character. Augmenting this core, the methodology additionally calls upon a suite of established forecasting engines: SARIMA, whose assignment is to resolve linear structure and seasonal regularities; LSTM, which shoulders the burden of capturing convoluted nonlinear relationships and dependencies that stretch over long temporal intervals; and Random Forest, which specializes in isolating patterns tied to specific features. The distinct analytical perspective supplied by each of these models collectively fortifies the robustness of the overall methodological edifice.

The outputs issuing from these separate models are subsequently merged into an integrated composite forecast, one designed to unify the respective strengths of the statistical and machine learning traditions under a single predictive umbrella. Leveraging wavelet preprocessing and Grey Markov analysis, the composite construct applies corrections that balance precision with dynamic adaptability, thereby bolstering forecast dependability. By virtue of its breadth, the approach is well-suited to confronting both linear and nonlinear phenomena embedded in the data, while remaining sufficiently supple to track the evolving contours of residual error patterns. The methodology is exceptionally well matched to contexts that place a premium on faithful deviation correction and on the capable handling of intricate patterning in time-series prediction tasks. **Table 5** places the forecasts generated with and without the RP stage side by side.

Table 5. Actual and next 12 predicted values (KW) for the proposed method without RP (SSRXL) and with RP (SSRXLR) deviation correction.

Point	12	11	10	9	8	7	6	5	4	3	2	1
Actual	0.699	0.989	1.732	0.664	0.625	0.59	0.59	0.846	1.84	0.752	0.646	0.65

© 2023 The Author(s). | Published by Institute of Smart Energy Systems Press

SSRXL	0.884	0.958	1.036	0.87	0.876	0.879	0.883	0.972	1.064	0.864	0.867	0.874
SSRXLR	0.701	0.989	1.714	0.795	0.708	0.612	0.612	0.883	1.73	0.768	0.775	0.782

A broad panel of competing techniques was assembled for benchmarking purposes: Linear Regression (LR), Random Forest (RF), Decision Tree (DT), Support Vector Machine (SVM), SARIMAX, Gated Recurrent Unit (GRU), Long Short-Term Memory (LSTM), and Deep Belief Network (DBN). The comparative findings are condensed in **Tables 6 and 7**, and a supplementary visual overview is supplied in **Figure 12.**

Table 6. Next 12 predicted (KW) Points by the Different Methods: (DBN, LSTM, SARIMAX, SSRXLR and the Input Data).

Method Point	Actual Data	SSRXLR	SARIMAX	LSTM	DBN
1	0.650	0.782	0.592	0.911	1.569
2	0.646	0.775	0.545	0.887	2.104
3	0.752	0.768	0.516	1.040	2.104
4	1.840	1.730	1.294	0.941	1.569
5	0.846	0.883	0.812	0.884	2.104
6	0.590	0.612	0.580	0.888	1.569
7	0.590	0.612	0.561	0.920	1.569
8	0.625	0.708	0.535	0.927	1.569
9	0.664	0.795	0.535	1.050	2.639
10	1.732	1.714	1.247	0.958	2.104
11	0.989	0.989	0.789	0.902	2.639
12	0.699	0.701	0.575	0.911	1.569

Table 7. Next 12 Predicted (KW) points by LR, RF, DT, SVM, GRU.

Method Point	XGBOOST	GRU	SVM	DT	RF	LR
1	0.871	0.938	0.621	0.951	0.853	1.634
2	0.699	0.923	0.602	0.279	0.703	1.610
3	0.637	0.901	0.569	0.513	0.643	1.576
4	1.968	1.112	0.665	3.180	1.963	1.941
5	0.89	0.953	0.637	0.946	0.892	1.658
6	0.643	0.899	0.565	0.513	0.643	1.573
7	0.632	0.902	0.570	0.513	0.631	1.577

© 2023 The Author(s). | Published by Institute of Smart Energy Systems Press

8	0.833	0.932	0.613	0.788	0.854	1.624
9	0.865	0.938	0.621	0.951	0.853	1.634
10	1.71	1.143	0.642	1.031	1.708	2.004
11	0.988	0.972	0.655	1.019	0.988	1.689
12	0.737	0.914	0.589	0.794	0.738	1.596

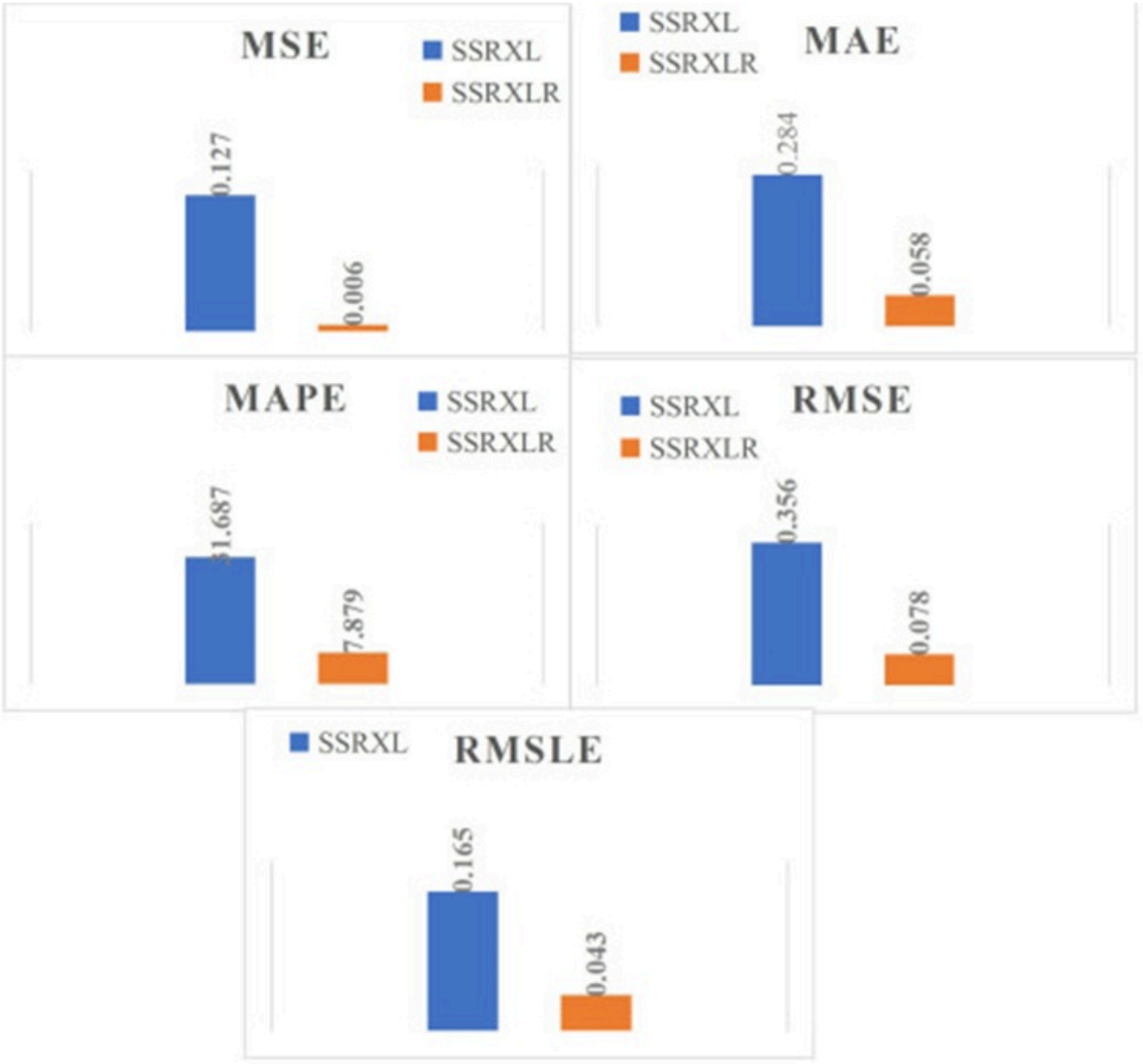

Figure 12. Comparison of SSRXL and SSRXLR using different metrics.

To validate that the residual-prediction (RP) model faithfully captures not solely the amplitude but also the polarity of the corrective term, actual residuals were evaluated as r_ac = Actual − SSRXL and predicted residuals as r_pr = SSRXLR − SSRXL across the twelve test points catalogued in **Table 5**. The Pearson correlation coefficient computed between the

© 2023 The Author(s). | Published by Institute of Smart Energy Systems Press

two sequences equals r = 0.9878 (P < 0.001). Such a near-identity, overwhelmingly significant positive correlation constitutes strong evidence that the RP model unfailingly anticipates residuals in the proper direction, ensuring that the corrective action of the SSRXLR step consistently compresses—never enlarges—the overall forecast error.

Five quantitative error indicators are enlisted to appraise the accuracy of the methods under examination: Mean Squared Error (MSE), Mean Absolute Error (MAE), Mean Absolute Percentage Error (MAPE), Root Mean Squared Logarithmic Error (RMSLE), and Root Mean Squared Error (RMSE). These six indices, whose mathematical definitions are supplied through the equations below, underpin the comparison pitting nine alternative techniques against the proposed approach (**Figure 13**, **Tables 6 and 7**).

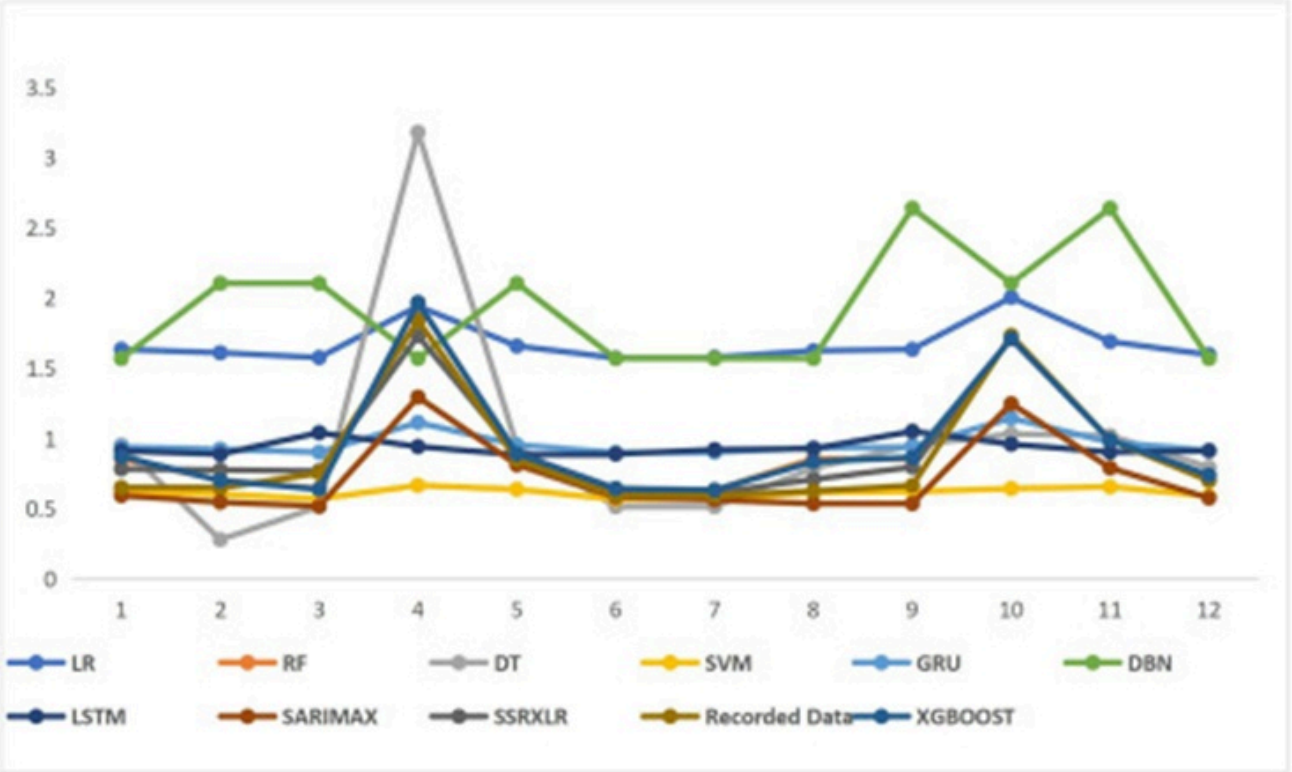

Figure 13. Comparison of Predicted Values (KW) by Different Methods for the Next 12 Points.

MSE [57] $$MSE = \frac{1}{N}\sum_{i=1}^{N}(A_i - F_i)^2 \quad (1)$$

MAE [58] $$MAE = \frac{1}{N}\sum_{i=1}^{N}|F_i - A_i| \quad (2)$$

MAPE [59] $$MAPE = \frac{1}{N}\sum_{i=1}^{N}\left|\frac{A_i - F_i}{A_i}\right| \times 100\% \quad (3)$$

RMSE [60] $$RMSE = \sqrt{\frac{1}{N} \times \sum_{i=1}^{N}(F_i - A_i)^2} \quad (4)$$

© 2023 The Author(s). | Published by Institute of Smart Energy Systems Press

RMSLE [61] $$\mathbf{RMSLE} = \sqrt{\frac{1}{N} \times \sum_{i=1}^{N} (\log(F_i + 1) - log(A_i + 1))^2} \quad (5)$$

R^2 [62] $$R^2 = 1 - \frac{\sum_{i=1}^{N} (Y - Y')^2}{\sum_{i=1}^{N} (Y - Y')} \quad (6)$$

The architectural logic of SSRXLR unfolds in two movements. The inaugural forecasting movement (SSRXL) deploys SARIMAX and XGBoost. Responsibility for modeling the linear autoregressive and moving-average skeleton—including its seasonal articulations—falls to SARIMAX. At the same time, the task of untangling the dense nonlinear interactions among exogenous drivers devolves to XGBoost. Between them, these two models manage to peel away most of the trend mass, seasonal architecture, and nonlinear effects from the raw load observations. The ensuing residual correction movement (RP) first mobilizes wavelet denoising to sift high-frequency noise from the meaningful low-frequency residual signature, then fields a Grey–Markov model—a tool with a demonstrated edge in probabilistic state-transition forecasting for sparse, short-duration series—paired with a lean SARIMA instance whose mission is to recover any residual linear or seasonal structure lingering in the de-noised error trace. Given that the error signal surviving the first movement is both compact and thinly populated, deploying heavyweight black-box learners would invite overfitting; the deliberately lightweight tandem adopted here provides a correction mechanism that is dynamic in operation yet frugal in complexity, homing in exclusively on what remains unexplained.

It should also be noted that any attempt to cycle the same model combination through the RP movement would be inherently duplicative: the patterns those models are capable of registering have, by this point, already been extracted. Hence the deliberate pivot to a different, more sharply focused pairing—one calibrated to maximize accuracy gains while holding the risk of overfitting firmly in check.

That SSRXLR surpasses the alternative forecasting approaches in accuracy is borne out by **Figure 14**. The source of this performance differential can be located in the contributions of the statistical modeling strand, which acted to steer the overall framework away from overfitting—a vulnerability to which machine learning techniques are notoriously prone—at the same time as the machine learning strand proved adept at disentangling the elaborate web of relationships woven through the data. A visual juxtaposition of actual observations against the forecasts issued by the three highest-performing methods is supplied in **Figure 15**. Over the prediction window, the Coefficient of Determination (R^2) was tallied at 0.97 for SSRXLR, 0.92 for RF, and 0.67 for SARIMAX. These numerical contrasts make plain that the proposed method outstrips all other evaluated techniques in terms of accuracy.

© 2023 The Author(s). | Published by Institute of Smart Energy Systems Press

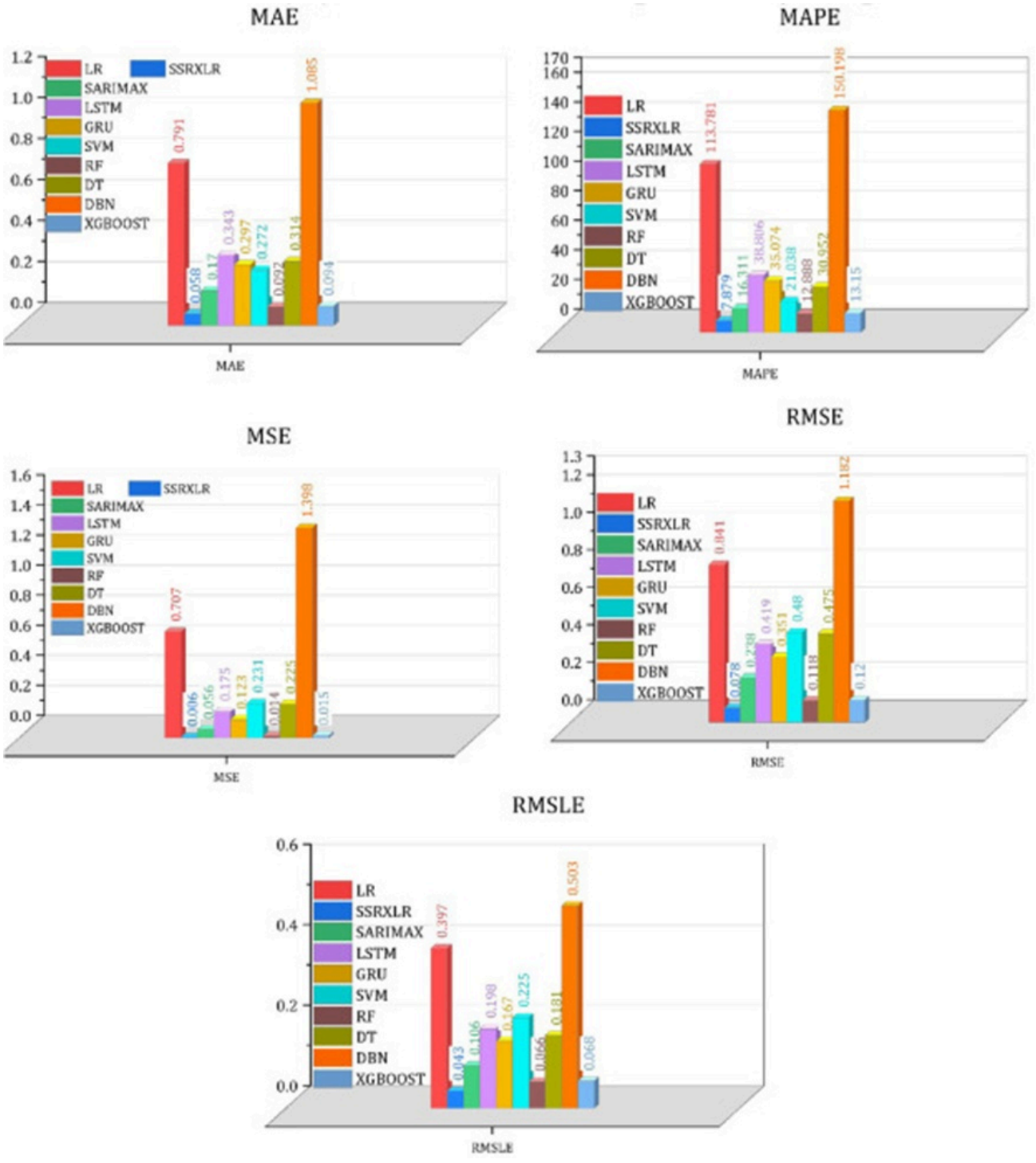

Figure 14. Evaluation of the nine methods for the case study data.

© 2023 The Author(s). | Published by Institute of Smart Energy Systems Press

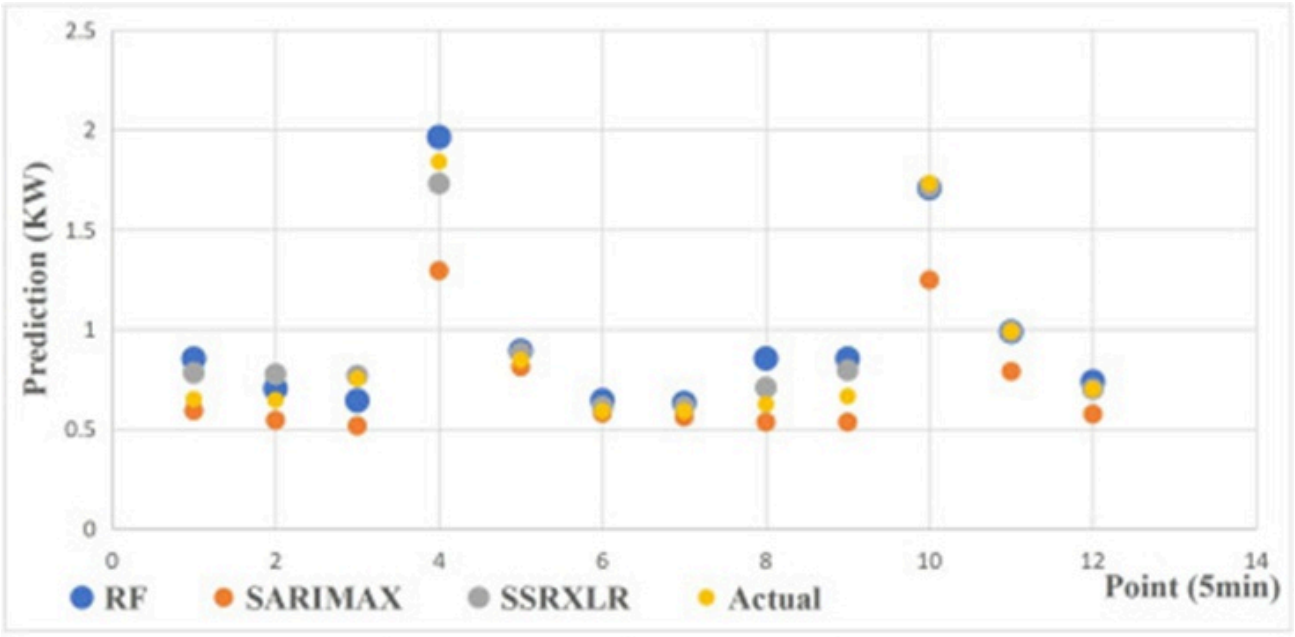

Method	R^2
SSRXLR	0.97
RF	0.92
SARIMAX	0.67

Figure 15. Comparison of actual and best three prediction methods for twelve points (KW).

What stands out immediately when examining the LR and DBN reference models is the extreme elevation of their MAPE readings. That this would be the case was fully anticipated: the rigidly linear mathematical structure of LR offers no mechanism for accommodating the nonlinear behaviors, seasonal oscillations, and holiday-driven anomalies embedded in high-resolution residential consumption traces, while the DBN variant fielded here—an unsupervised deep belief network—lacks the dedicated architectural provisions that such pattern capture would necessitate. A strikingly different picture emerges for SARIMAX, whose MAPE registers at a notably depressed level. The parameter space defined by (p, d, q) and (P, D, Q, s) was exhaustively traversed in a grid search, with retention governed by the AIC minimum. The dataset's own properties—its emphatic seasonal periodicity coupled with relatively quiescent residuals—create an environment in which a well-specified SARIMAX flourishes, and this alignment underlies the model's superior error characteristics in the present forecasting exercise.

The architectural blueprints and hyperparameter selections that define each baseline model within our comparative framework are brought together in **Table 8.**

Table 8. Baseline model architectures and hyperparameter settings.

Model	Structure/Hyperparameter settings
LR	Ordinary least squares regression; no regularization applied; solver = auto
SARIMAX	(p,d,q) = (1,1,1), seasonal order (P, D, Q, s) = (1,1,1,24), trend = constant (c), estimated via maximum likelihood
LSTM	Two stacked LSTM layers with 50 units eachdropout = 0.2batch size = 32, epochs = 100optimizer = Adam (learning rate = 0.001)

© 2023 The Author(s). | Published by Institute of Smart Energy Systems Press

GRU	Kernel = RBFC = 1.0, γ = “scale”, epsilon = 0.1 (ε-SVR formulation)
SVM	n_estimators = 100, max depth = 10min samples split = 2, criterion = MSE
RF	criterion = MSE, max depth = 5min samples leaf = 1
DT	criterion = MSE, max depth = 5min samples leaf = 1
DBN	3-layer architecture (input → 64 → 32 → output)learning rate = 0.01batch size = 64, epochs = 50contrastive divergence = 1
XGBOOST	n_estimators = 100, max depth = 5learning rate = 0.1subsample = 0.8, colsample_bytree = 0.8objective = reg:squared error

Practical Applications and Operational Benefits

To establish the operational relevance of SSRXLR, its predictive capability was tested on a full year of household load readings collected at five-minute granularity in Las Vegas, NV, and the resulting twelve-step-ahead forecasts were measured against those from Random Forest, SARIMAX, and XGBoost. A battery of error indices—MAE, MAPE, RMSE, RMSLE, and MSE—was pressed into service to construct a thorough evaluative portrait. The picture that emerges from this analysis is one in which the heightened accuracy of SSRXLR cascades into a series of concrete operational advantages for those charged with managing the grid: peak-load dispatch can be scheduled with sharper precision, tariff offers can be calibrated more advantageously, the buffer of reserve capacity can be drawn down, and the incorporation of stochastic renewable output can proceed with less friction—benefits whose collective effect is to compress operational costs while simultaneously stiffening system-wide dependability.

Although the empirical grounding of SSRXLR rests on load observations from Las Vegas, nothing in its constitution ties it to that locale. The design is deliberately modular, interlocking SARIMAX, tree-based ensemble methods, LSTM, and residual correction into a configuration that lends itself to reconfiguration across geographic and load-type boundaries. By re-estimating the model on locally appropriate historical sequences and exogenous drivers—meteorological readings, holiday schedules, and consumption signatures being prime examples—adopters can ready SSRXLR for short-horizon forecasting duties in any national or climatological setting.

The available data were partitioned according to an 80/20 scheme, the dominant share being allocated to training and the remainder held out for validation, a division calculated to promote sound model construction while insulating the evaluation from bias. Short-Term Load Forecasting (STLF) constitutes the central preoccupation of this research—a function that sits at the very heart of live operational choice-making and grid orchestration—and for this reason predictive effort is concentrated on the coming 12 temporal increments, each marking a 5-minute interval, collectively accounting for one hour of energy consumption ahead. Such a forecast window is precisely matched to the demands of near-term energy dispatch and regulation, where resolving abrupt demand swings requires fine temporal discrimination. Extending the gaze to more distant horizons unquestionably yields perspectives valuable for higher-level planning. Still, our methodological commitment is to high-fidelity, short-range prediction of the sort that carries immediate weight in operational grid settings. Evidence of the model’s capacity to extend beyond the immediate horizon was sought through testing over multi-day intervals. Forecasts spanning the concluding three days of 2022 (at the native 5-minute resolution, amounting to 864 individual points) are displayed in **Figure 16** and quantified in **Table 9.**

© 2023 The Author(s). | Published by Institute of Smart Energy Systems Press

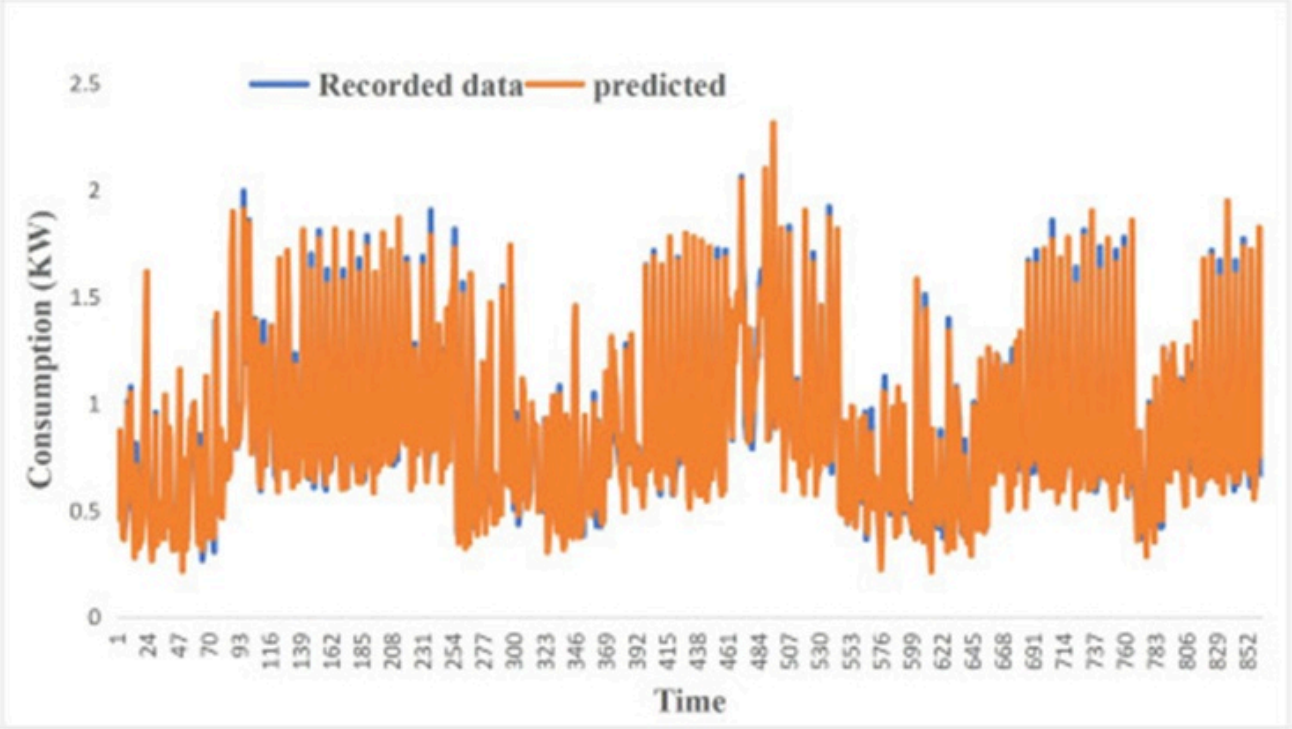

Figure 16. Comparison of actual (Recorded) and predicted consumption values (KW) for the last 3 days of 2022.

Table 9. Evaluation of the last 3 days (864 points) for the case study data.

Metric	MAE	MSE	MAPE	RMSE	RMSLE
Value	0.0456	0.00328	6.39 %	0.0573	0.0326

A detailed treatment and interpretive discussion of forecasting over medium and extended timescales falls outside the boundaries of the present contribution.

Conclusion

The contribution made by this paper takes the form of a pioneering hybrid methodology for electrical load forecasting, one in which machine learning and statistical traditions—Seasonal Autoregressive Integrated Moving Average Exogenous, Random Forest, Extreme Gradient Boosting, and Long Short-Term Memory—figure prominently. The resulting instrument is purpose-built to raise the standard of fine-grained, short-horizon load projection. It capitalizes on machine learning's aptitude for surfacing concealed relationships and ingesting expansive datasets, while drawing strength from the lucidity, interpretability, and sound mathematical footing that are the hallmarks of statistical techniques.

Benchmarked against a field of eight alternative approaches—encompassing both machine learning and parametric statistical formulations, specifically Linear Regression, Random Forest, Decision Tree, Support Vector Machine, Gated Recurrent Unit, Deep Belief Network, Long Short-Term Memory, and Seasonal Autoregressive Integrated Moving Average Exogenous—the proposed method registers performance advances of considerable magnitude when assessed through the lenses of RMSLE and MAPE. The RMSLE and MAPE figures recorded are, in order: 0.39, 0.06, 0.18, 0.22, 0.16, 0.5, 0.19, 0.1; and 113.7%, 12.8%, 30.9%, 21%, 35.1%, 150.2%, 38.8%, 16.3%. From these numbers, one may conclude that

© 2023 The Author(s). | Published by Institute of Smart Energy Systems Press

the union of AI-grounded modeling with disciplined feature curation delivers performance that is decisively superior to that of the reference set, and that the resulting framework constitutes a scalable and robust asset for enhancing grid dependability, energy management practice, and operational planning.

The inclusion of additional processing layers distinguishes the proposed method. Through the concerted deployment of analysis of variance, Minimum Redundancy Maximum Relevance and Minimum Synergy, Correlation Matrix, and the Chi-Square Test, a compact set of driving features was identified: temperature, sea-level pressure, dew point, and solar radiation. A holiday coefficient was additionally quantified, a step that permitted the smoothing of trend components and the alignment of seasonal structure by normalizing each month to a uniform 31-day span. A deviation correction module was subsequently introduced to project the residual sequence across the next 12 points with fidelity.

The empirical locus of the study was a single-family dwelling in the Summerlin district of Las Vegas, Nevada, USA. The short-term predictive outcomes (covering the forward hour) document a meaningful compression of error when set against the comparator methods. RMSLE improvement, expressed in percentage terms, amounts to 89.17% against linear regression, 34.85% against random forest, 76.24% against decision tree, 80.89% against support vector machine, 74.25% against gated recurrent unit, 91.45% against deep belief network, 78.28% against long short-term memory, and 59.43% against seasonal autoregressive integrated moving average exogenous. The hybrid remainder prediction component, which combines the Wavelet Residual Modified Grey Forecasting model, the Grey-Markov model, Long Short-Term Memory, Random Forest, and SARIMA, provides a further increment in accuracy. For all its demonstrated power, the proposed method carries with it certain burdens, notably the complexity and resource cost of implementation, together with the depth of computational science expertise it presupposes.

Acknowledgements

None

Conflict of interest

None

Financial support

None

Ethics statement

None

Received: 16 May 2022 Revised: 24 Jul 2022 Accepted: 10 Aug 2022
Published online: 15 June 2023

Rights and permissions

Open Access The author(s) retain copyright. This article is licensed under the Creative Commons Attribution-NonCommercial-ShareAlike 4.0 International License. It may be shared and adapted for non-commercial purposes with appropriate attribution, an indication of changes, and

distribution of adaptations under the same license. Third-party material may be subject to separate terms identified in its credit line. View the license at https://creativecommons.org/licenses/by-nc-sa/4.0/.

References

1. Widmer F, Nowak S, Bowler B, Huber P, Papaemmanouil A. Data-driven comparison of federated learning and model personalization for electric load forecasting. Energy AI. 2023;14:100253. https://doi.org/10.1016/j.egyai.2023.100253.

2. Miraki A, Parviainen P, Arghandeh R. Probabilistic forecasting of renewable energy and electricity demand using graph-based Denoising Diffusion Probabilistic model. Energy AI. 2025;19:100459. https://doi.org/10.1016/j.egyai.2024.100459.

3. Pallonetto F, Jin C, Mangina E. Forecast electricity demand in commercial building with machine learning models to enable demand response programs. Energy AI. 2022;7:100121. https://doi.org/10.1016/j.egyai.2021.100121.

4. Baesmat KH, Shiri A. A new combined method for future energy forecasting in electrical networks. Int Trans Electr Energy Syst. 2019;29(3):e2749. https://doi.org/10.1002/etep.2749.

5. Baesmat KH. Impedance analysis of adaptive distance relays using machine learning. In: Latifi S, ed. ITNG 2024: 21st International Conference on Information Technology-New Generations. Springer; 2024:1456. https://doi.org/10.1007/978-3-031-56599-1_57.

6. Li B, Mostafavi A. Unraveling fundamental properties of power system resilience curves using unsupervised machine learning. Energy AI. 2024;16:100351. https://doi.org/10.1016/j.egyai.2024.100351.

7. Ibraheem R, Cannings TI, Sell T, dos Reis G. Robust survival model for the prediction of Li-ion battery lifetime reliability and risk functions. Energy AI. 2025;19:100465. https://doi.org/10.1016/j.egyai.2024.100465.

8. Li X, Maréchal F. Deep excavation of the impact from endogenous and exogenous uncertainties on long-term energy planning. Energy AI. 2023;11:100219. https://doi.org/10.1016/j.egyai.2022.100219.

9. Baesmat KH, Masoudipour I, Samet H. Improving the performance of short-term load forecast using a hybrid artificial neural network and artificial bee colony algorithm. IEEE Can J Electr Comput Eng. 2021;44(3):275-82. https://doi.org/10.1109/ICJECE.2021.3056125.

10. Zareipour H, Canizares CA, Bhattacharya K. Economic impact of electricity market price forecasting errors: a demand-side analysis. IEEE Trans Power Syst. 2010;25(1):254-62. https://doi.org/10.1109/TPWRS.2009.2030380.

11. Weron R. Electricity price forecasting: a review of the state-of-the-art with a look into the future. Int J Forecast. 2014;30(4):1030-81. https://doi.org/10.1016/j.ijforecast.2014.08.008.

12. Billé AG, Gianfreda A, Del Grosso F, Ravazzolo F. Forecasting electricity prices with expert, linear, and nonlinear models. Int J Forecast. 2023;39(2):570-86. https://doi.org/10.1016/j.ijforecast.2022.01.003.

© 2023 The Author(s). | Published by Institute of Smart Energy Systems Press

13. Mahmood S, Sun H, Alhussan AA, Iqbal A, El-kenawy EM. Active learning-based machine learning approach for enhancing environmental sustainability in green building energy consumption. Sci Rep. 2024;14:19894. https://doi.org/10.1038/s41598-024-70729-4.

14. Ramnath GS, Harikrishnan R, Muyeen SM, Kotecha K. Household electricity consumption prediction using database combinations, ensemble and hybrid modeling techniques. Sci Rep. 2024;14:22891. https://doi.org/10.1038/s41598-024-57550-9.

15. Shaqour A, Ono T, Hagishima A, Farzaneh H. Electrical demand aggregation effects on the performance of deep learning-based short-term load forecasting of a residential building. Energy AI. 2022;8:100141. https://doi.org/10.1016/j.egyai.2022.100141.

16. Chen Y, Gong W, Obrecht C, Kuznik F. A review of machine learning techniques for building electrical energy consumption prediction. Energy AI. 2025;21:100518. https://doi.org/10.1016/j.egyai.2025.100518.

17. Baur L, Ditschuneit K, Schambach M, Kaymakci C, Wollmann T, Sauer A. Explainability and interpretability in electric load forecasting using machine learning techniques – A review. Energy AI. 2024;16:100358. https://doi.org/10.1016/j.egyai.2024.100358.

18. Antonesi G, Cioara T, Anghel I, Papias I, Michalakopoulos V, Sarmas E, et al. Hybrid transformer model with liquid neural networks and learnable encodings for buildings' energy forecasting. Energy AI. 2025;20:100489. https://doi.org/10.1016/j.egyai.2025.100489.

19. Baesmat KH, Latifi S. A new hybrid method for electrical load forecasting based on deviation correction and MRMRMS. In: Selvaraj H, Chmaj G, Zydek D, eds. Advances in Systems Engineering. ICSEng 2023. Springer; 2023:761. https://doi.org/10.1007/978-3-031-40579-2_29.

20. Baesmat KH. SP-RF-ARIMA: a sparse random forest and ARIMA hybrid model for electric load forecasting. Glob Energy Interconnect. 2025. https://doi.org/10.1016/j.gloei.2025.04.003.

21. Baesmat KH, Farrokhi Z, Chmaj G, Regentova EE. Parallel multi-model energy demand forecasting with cloud redundancy: leveraging trend correction, feature selection, and machine learning. Forecasting. 2025;7:25. https://doi.org/10.3390/forecast7020025.

22. Song Z, Xiao F, Chen Z, Madsen H. Probabilistic ultra-short-term solar photovoltaic power forecasting using natural gradient boosting with attention-enhanced neural networks. Energy AI. 2025;20:100496.

23. Liu B, Nowotarski J, Hong T, Weron R. Probabilistic load forecasting via quantile regression averaging on sister forecasts. IEEE Trans Smart Grid. 2017;8(2):730-7. https://doi.org/10.1109/TSG.2015.2437877.

24. Kuster C, Rezgui Y, Mourshed M. Electrical load forecasting models: a critical systematic review. Sustain Cities Soc. 2017;35:257-70. https://doi.org/10.1016/j.scs.2017.08.009.

25. Zhang GP. Time series forecasting using a hybrid ARIMA and neural network model. Neurocomputing. 2003;50:159-75. https://doi.org/10.1016/S0925-2312(01)00702-0.

26. Haq MR, Ni Z. A new hybrid model for short-term electricity load forecasting. IEEE Access. 2019;7:125413-23. https://doi.org/10.1109/ACCESS.2019.2937222.

27. Xu C, Sun Y, Du A, Gao D. Quantile regression based probabilistic forecasting of renewable energy generation and building electrical load: a state of the art review. J Build Eng. 2023;79:107772.

© 2023 The Author(s). | Published by Institute of Smart Energy Systems Press

https://doi.org/10.1016/j.jobe.2023.107772.

28. Guo J, He H, Sun C. ARIMA-based road gradient and vehicle velocity prediction for hybrid electric vehicle energy management. IEEE Trans Veh Technol. 2019;68(6):5309-20. https://doi.org/10.1109/TVT.2019.2912893.

29. Wasesa M, Tiara AR, Afrianto MA, Ramadhan FI, Haq IN, Pradipta J. SARIMA and artificial neural network models for forecasting electricity consumption of a microgrid based educational building. In: 2020 IEEE International Conference on Industrial Engineering and Engineering Management (IEEM). IEEE; 2020:210-4. https://doi.org/10.1109/IEEM45057.2020.9309943.

30. Jamali H, Karimi A, Haghighizadeh M. A new method of cloud-based computation model for mobile devices: energy consumption optimization in mobile-to-mobile computation offloading. In: Proceedings of the 6th International Conference on Communications and Broadband Networking (ICCBN '18). ACM; 2018:32-7. https://doi.org/10.1145/3193092.3193103.

31. Islam MS, Alam MM, Ahamed A, Meerza SIA. Prediction of diabetes at early stage using interpretable machine learning. In: SoutheastCon 2023. IEEE; 2023:261-5. https://doi.org/10.1109/SoutheastCon51012.2023.10115152.

32. Deng Z, Wang B, Xu Y, Xu T, Liu C, Zhu Z. Multi-scale convolutional neural network with time-cognition for multi-step short-term load forecasting. IEEE Access. 2019;7:88058-71. https://doi.org/10.1109/ACCESS.2019.2926137.

33. Lin W, Wu D, Boulet B. Spatial-temporal residential short-term load forecasting via graph neural networks. IEEE Trans Smart Grid. 2021;12(6):5373-84. https://doi.org/10.1109/TSG.2021.3093515.

34. Mir AA, Khan ZA, Altmimi A, Badar M, Ullah K, Imran M. Systematic development of short-term load forecasting models for the electric power utilities: the case of Pakistan. IEEE Access. 2021;9:140281-97. https://doi.org/10.1109/ACCESS.2021.3117951.

35. Sharma A, Jain SK. A novel two-stage framework for mid-term electric load forecasting. IEEE Trans Ind Inform. 2024;20(1):247-55. https://doi.org/10.1109/TII.2023.3259445.

36. Shaikh AK, Nazir A, Khan I, Shah AS. Short term energy consumption forecasting using neural basis expansion analysis for interpretable time series. Sci Rep. 2022;12:22562. https://doi.org/10.1038/s41598-022-26499-y.

37. Azeem A, Ismail I, Jameel SM, Harindran VR. Electrical load forecasting models for different generation modalities: a review. IEEE Access. 2021;9:142239-63. https://doi.org/10.1109/ACCESS.2021.3120731.

38. Lambert G, Hamrouche B, de Vilmarest J. Frugal day-ahead forecasting of multiple local electricity loads by aggregating adaptive models. Sci Rep. 2023;13:15784. https://doi.org/10.1038/s41598-023-42488-1.

39. Nie H, Liu G, Liu X, Wang Y. Hybrid of ARIMA and SVMs for short-term load forecasting. Energy Procedia. 2012;16(Pt C):1455-60. https://doi.org/10.1016/j.egypro.2012.01.229.

40. Bilgili M, Pinar E. Gross electricity consumption forecasting using LSTM and SARIMA approaches: a case study of Türkiye. Energy. 2023;284:128575. https://doi.org/10.1016/j.energy.2023.128575.

© 2023 The Author(s). | Published by Institute of Smart Energy Systems Press

41. Zhang Z, Zhang Q, Liang H, Gorbani B. Optimizing electric load forecasting with support vector regression/LSTM optimized by flexible Gorilla troops algorithm and neural networks a case study. Sci Rep. 2024;14:22092. https://doi.org/10.1038/s41598-024-73893-9.

42. Abedinia O, Amjady N, Zareipour H. A new feature selection technique for load and price forecast of electrical power systems. IEEE Trans Power Syst. 2017;32(1):62-74. https://doi.org/10.1109/TPWRS.2016.2556620.

43. Visual Crossing (2022) Weather Data. Visual Crossing. www.visualcrossing.com/, 2022.

44. Jamali H, Dascalu SM, Harris FC. AI-driven analysis and prediction of energy consumption in NYC's municipal buildings. In: 2024 IEEE/ACIS 22nd International Conference on Software Engineering Research, Management and Applications (SERA). IEEE; 2024:277-83. https://doi.org/10.1109/SERA61261.2024.10685594.

45. Jamali H, Dascalu SM, Harris FC. Fostering joint innovation: a global online platform for ideas sharing and collaboration. In: Latifi S, ed. ITNG 2024: 21st International Conference on Information Technology-New Generations. Springer; 2024:1456. https://doi.org/10.1007/978-3-031-56599-1_40.

46. Farrokhi Z, Kalhor A, Masouleh MT. Implementation and evaluation of object identification techniques on Nao robot platform. Int J Mechatron Electr Comput Technol. 2018;8(29):3947-58. https://aeuso.org/includes/files/articles/Vol8_Iss29_3947-3958_Implementation_and_Evaluation_of_Ob.pdf

47. Habib AKMR, Alam MM, Islam MR. Design of a mobile aeration system for aquaculture and proof of concept. In: 2021 International Conference on Computer, Communication, Chemical, Materials and Electronic Engineering (IC4ME2). IEEE; 2021:1-4. https://doi.org/10.1109/IC4ME253898.2021.9768594.

48. Jamali H, Shill PC, Feil-Seifer D, Harris FC, Dascalu SM. A schedule of duties in the cloud space using a modified salp swarm algorithm. In: Puthal D, Mohanty S, Choi BY, eds. Internet of Things. IFIPIoT 2023. Springer; 2024;683. https://doi.org/10.1007/978-3-031-45878-1_5.

49. Shill PC, Wu R, Jamali H, Hutchins B, Dascalu S, Harris FC. WIP: development of a student-centered personalized learning framework to advance undergraduate robotics education. In: 2023 IEEE Frontiers in Education Conference (FIE). IEEE; 2023:1-5. https://doi.org/10.1109/FIE58773.2023.10343234.

50. Wu R, Dascalu S, Zhu Z, Feil-Seifer D, Ringler MC, Hutchins BC, et al. Board 413: undergraduate robotics education with general instructors using a student-centered personalized learning framework. In: 2024 ASEE Annual Conference & Exposition. 2024. –47002 https://doi.org/10.18260/1-2.

51. Nakip M, Karakayali K, Güzelış C, Rodoplu V. An end-to-end trainable feature selection-forecasting architecture targeted at the internet of things. IEEE Access. 2021;9:104011-28. https://doi.org/10.1109/ACCESS.2021.3092228.

52. Chetry BP, Kar B. Online signature verification using Chi-Square (χ2) feature selection and SVM classifier. In: 2024 6th International Conference on Energy, Power and Environment (ICEPE). IEEE; 2024:1-6. https://doi.org/10.1109/ICEPE63236.2024.10668917.

53. Farrokhi Z, Baesmat K, Regentova E. Enhancing urban intelligence energy management: innovative load forecasting techniques for electrical networks. J Power Energy Eng. 2024;12:72-88. https://doi.org/10.4236/jpee.2024.1211005.

© 2023 The Author(s). | Published by Institute of Smart Energy Systems Press

54. Xiao L, Chen X, Wang H. Calculation and realization of new method grey residual error correction model. PLoS ONE. 2021;16(7):e0254154. https://doi.org/10.1371/journal.pone.0254154.

55. Kim D, Cho Y, Kim D, Park C, Choo J. Residual correction in real-time traffic forecasting. In: Proceedings of the 31st ACM International Conference on Information & Knowledge Management. ACM; 2022:962-71. https://doi.org/10.1145/3511808.3557432.

56. Sun J. Medium and long-term power load forecasting based on Grey Markov correction model. Int J Front Sociol. 2022;4(5):53-62. https://doi.org/10.25236/IJFS.2022.040511.

57. Wen X, Liao J, Niu Q, Bao Y. Deep learning-driven hybrid model for short-term load forecasting and smart grid information management. Sci Rep. 2024;14:13720. https://doi.org/10.1038/s41598-024-63262-x.

58. Qinghe Z, Wen X, Boyan H, Junlong F. Optimised extreme gradient boosting model for short term electric load demand forecasting of regional grid system. Sci Rep. 2022;12:19282. https://doi.org/10.1038/s41598-022-22024-3.

59. Zhao M, Guo G, Fan L, Han L, Yu Q, Wang Z. Short-term natural gas load forecasting based on EL-VMD-Transformer-ResLSTM. Sci Rep. 2024;14:20343. https://doi.org/10.1038/s41598-024-70384-9.

60. Joshi B, Singh VK, Vishwakarma DK, Ghorbani MA, Kim S, Gupta S. A comparative survey between cascade correlation neural network (CCNN) and feedforward neural network (FFNN) machine learning models for forecasting suspended sediment concentration. Sci Rep. 2024;14:10638. https://doi.org/10.1038/s41598-024-61339-1.

61. Sarker B, Chakraborty S, Čep R, Kalita K. Development of optimized ensemble machine learning-based prediction models for wire electrical discharge machining processes. Sci Rep. 2024;14:23299. https://doi.org/10.1038/s41598-024-74291-x.

62. Ahmed T, Powner MB, Qassem M, Kyriacou PA. Rapid optical determination of salivary cortisol responses in individuals undergoing physiological and psychological stress. Sci Rep. 2024;14:31578. https://doi.org/10.1038/s41598-024-69466-5.

© 2023 The Author(s). | Published by Institute of Smart Energy Systems Press